交通部中央氣象局

委託研究計畫(期末)成果報告

結合感測、系統識別及健康診斷技術
探討橋梁結構破壞預警模式及機制（II）

Integration of sensing, system identification and health monitoring technologies for damage prognosis of bridges (II)

計畫類別：□氣象　□海象　■地震

計畫編號： MOTC-CWB-100-E-06

執行期間： 101 年 1 月 1 日至 101 年 12 月 31 日

計畫主持人：羅俊雄 (台灣大學土木工程學系教授)

執行機構：台大工學院地震中心

中華民國 101 年 11 月 25 日

政府研究計畫期末報告摘要資料表

<table>
<tr><td>計畫中文名稱</td><td colspan="3">結合感測、系統識別及健康診斷技術探討橋梁結構破壞預警模式及機制（II）</td></tr>
<tr><td>計畫編號</td><td colspan="3">MOTC-CWB-100-E-06</td></tr>
<tr><td>主管機關</td><td colspan="3">交通部中央氣象局</td></tr>
<tr><td>執行機構</td><td colspan="3">台大工學院地震中心</td></tr>
<tr><td>年度</td><td>101</td><td>執行期間</td><td>中華民國 101 年 11 月 25 日</td></tr>
<tr><td>本期經費
（單位：千元）</td><td colspan="3">900</td></tr>
<tr><td rowspan="2">執行進度</td><td>預定（%）</td><td>實際（%）</td><td>比較（%）</td></tr>
<tr><td>100</td><td>100</td><td>100</td></tr>
<tr><td rowspan="2">經費支用</td><td>預定(千元)</td><td>實際(千元)</td><td>支用率（%）</td></tr>
<tr><td>900</td><td>900</td><td>100</td></tr>
<tr><td rowspan="4">研究人員</td><td>計畫主持人</td><td>協同主持人</td><td>研究助理</td></tr>
<tr><td rowspan="3">羅俊雄</td><td>林沛暘</td><td>曾敏軒</td></tr>
<tr><td>高清雲</td><td>劉建榮</td></tr>
<tr><td></td><td></td></tr>
<tr><td>報告頁數</td><td>40 頁</td><td>使用語言</td><td>中文摘要英文內容</td></tr>
<tr><td>中英文關鍵詞</td><td colspan="3">結構健康診斷，即時損壞評估，無線感測系統。
(Structural Health Monitoring, On-line damage detection, wireless sensing system)</td></tr>
<tr><td>研究目的</td><td colspan="3">1. 提升及改善現有橋梁監測系統並配合流域之監測，以最適化流域監測及橋梁監測，建置有效的橋梁監測系統 。
2. 改善及研發有效的橋梁監測用感應器，並配合監測系統之可靠度分析，提昇橋梁防災能力。</td></tr>
<tr><td>研究成果</td><td colspan="3">1. 建立 Real Time 橋梁監測系統，即時回報橋梁現況。，可迅速進行建物之健康診斷，提供預警效果。
2. 實際應用於關渡橋及牛門橋之振動監測。</td></tr>
<tr><td>具體落實應用情形</td><td colspan="3">1. 系統雛型建置於臺大土木新大樓，進行測試。
2. 實際應用於關渡橋之常態監測並探討環境因素對橋梁振動頻率之影響。</td></tr>
<tr><td>計畫變更說明</td><td colspan="3">無</td></tr>
<tr><td>落後原因</td><td colspan="3">無</td></tr>
<tr><td>檢討與建議
（變更或落後之因應對策）</td><td colspan="3"></td></tr>
</table>

（以下接全文報告）

結合感測、系統識別及健康診斷技術
探討橋梁結構破壞預警模式及機制(II)

計畫主持人: 羅俊雄 (台灣大學土木工程學系教授)

計畫摘要概括說明(ABSTRACT)：

台灣由於地理環境特殊，經常受到天然災害的襲擊，其中包括地震、颱風、洪水與土石流等等，因此重要的基礎建設，例如校舍、橋梁、與隧道等等，其安全性以及耐久性便成為相當重要的議題。以橋梁為例，近年來有許多橋梁在颱風侵襲期間因為暴漲的溪水或土石流沖蝕，導致橋面板的陷落以及橋體的損壞，造成人命傷亡與經濟損失。因此當務之急除了針對現有橋梁進行整體安全性評估之外，將來更需要發展準確與可靠的橋梁監測系統，對橋梁的安全性進行監測，並在橋梁損害發生與倒塌之前提供預警訊息，以減少人命與經濟的損失。為了實踐以振動量測為基礎的橋梁安全監測平台，先前之研究以無線感測模組對宜蘭牛鬥橋及關渡橋進行長期監測，並採用遞迴性隨機子空間分析法(Recursive Stochastic Subspace Identification, RSSI)對收集之量測訊號進行分析，達到橋梁監測之目的。

本研究之目的在發展一套有效且快速之結構健康診斷之工具，去進行正在使用中之結構(含橋梁)，利用常態反應之量測資料，進行模態分析（Operational Model Analysis, OMA）及其特徵(features）判別方法之研究。並利用所識別之特徵，同時亦一併進行該結構之快速損壞檢測。對收集到之量測訊號之系統識別方法，以達到即時(almost real-time)及上線(on-line) 分析方式進行，配合遞迴性隨機子空間分析法(Recursive Stochastic Subspace Identification, RSSI-DATA &RSSI-COV)進行識別外，探討以減少運算時間為主，達到即時監測之目的。研究中並針對 SSI 之方法探討分析模式所使用之參數不確定性造成對識別結果之變異進行討論，以期正確識別結構物之動態特徵。而在快速損壞檢測之研究，以探討不同損壞指標對結構損壞檢測之敏銳度為主。研究方法將應用於實驗室縮尺橋梁實驗之沖刷試驗，同時亦嘗試在現地進行橋梁測試，整合此分析軟體於無線感測器內，進行橋梁結構之微振量測。以期發展準確與可靠的橋梁監測系統，對橋梁的安全性進行監測，並在橋梁損害發生與倒塌之前提供預警訊息。

本期中報告首先將針對探討不同損壞指標對結構損壞檢測之敏銳度為主。研究中推導出四種損傷指標，強調以移動窗函數技術以快速及振動反應量測記錄進行分析，即時提供預警訊息。研究中亦以大型水工實驗進行驗証。期末報告則包含橋梁常態監測之振動頻率與環境因素之關聯。並將此技術應用於關渡橋之振動量測上。

Part 1: Modeling of Environmental Effects for Vibration-based SHM Using Recursive Stochastic Subspace Identification Analysis

Part 2: Develop On-Line Damage Detection Methods of Bridges under Abnormal Conditions

報告內容分兩部份：常態監測及異常狀態下損壞評估。整體架構如圖一所示之研究架構。

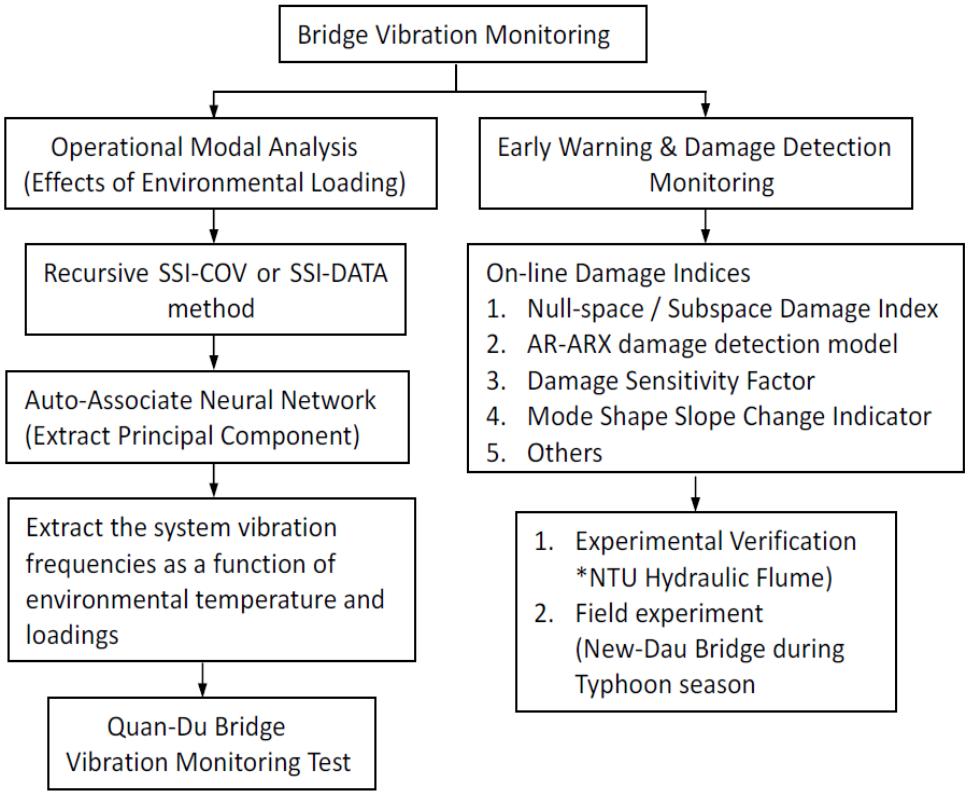

圖一：研究報告分兩部份：常態監測及異常狀態下損壞評估。

Part 1:

Modeling of Environmental Effects for Vibration-based SHM Using Recursive Stochastic Subspace Identification Analysis

Abstract This paper deals with the problem of a bridge structure identification using output-only vibration measurements under changing environmental conditions. Two key issues of a real-life monitoring system are addressed through analysis. The first issue is the identification of structural dynamic characteristics directly from measurements under operating conditions. The covariance- driven recursive stochastic subspace identification (RSSI-COV) algorithm is applied to extract the system dynamic characteristics. The second issue is to distinguish the system dynamic features caused by abnormality from those caused by environmental and operational variations, such as temperature, and traffic loading. In this study a solution is proposed to model and remove the uncertainty due to environmental effects from the identified system dynamic characteristics from on-going measurements. Nonlinear principal component analysis incorporated with AANN is employed to distinguish the dynamic feature changes caused by abnormality from those caused by environmental and operational variation (i.e. ambient temperature and traffic loadings). Finally, field experiment of a bridge is conducted. The variation of the identified system natural frequencies was discussed by using the proposed method.

1. Introduction

Identification of modal parameters using ambient excitation is more feasible to large engineering structures. Those responses caused by ambient excitation can be employed in the field of structural health monitoring (SHM) to evaluate the health condition of an in-service structure. Generally, the aim of vibration-based SHM methods is to detect the appearance of damages by evaluating changes in the identified vibration characteristics. In the past, many vibration-based methods were developed to monitor structural safety. A common structural monitoring approach is the modal analysis, which using output-only system identification technique to identify structural modal frequency, modal damping ratio and mode shape from vibration data. The extraction of features from these measurements and the analysis of these features to determine the current state of health of the system using spaced measurement provide a tool for SHM and damage detection.

Stochastic Subspace Identification (SSI) technique is a well known multivariate identification technique by using the output-only measurements which can provide the modal analysis of structures under operating condition. The SSI technique proved to be numerically stable, robust to noise perturbation and suitable for conducting non-stationarity of the ambient excitations. The stochastic realization algorithm mainly focused on SSI-DATA and was fully enhanced by Van Overschee and De Moor [1] and Peeters, Bart [2-4]. Application of the SSI-DATA algorithm to

investigate the dynamic characteristics of bridge and aeronautical structures had been studied [5-7]. As opposed to SSI-DATA the SSI-COV algorithm avoids the computation of orthogonal projection; instead, it is replaced by converting raw time histories in co-variances of the so-called Toeplitz matrix, from which the system dynamic characteristics can be extracted.

Different from the off-line analysis, the on-line system identification and damage detection based on the measured vibration data has also received considerable attention recently. Generally, the recursive Data-driven subspace algorithm is the most widely used [8,9]. In order to reduce the effect of noise on the results of identification, some filtering techniques need to be used in recursive SSI so as to enhance the early emergence of a stable diagram for the identifiable modes and allows finding the best choice of system order. Therefore, the recursive stochastic realization by the classical Covariance-driven SSI algorithm (RSSI-COV) was proposed in [10]. In this paper the RSSI-COV method is applied to extract the time-varying system natural frequencies of Guan-Du Bridge. Through the continuous monitoring of the bridge the identified system natural frequencies of the bridge caused by abnormality from those caused by environmental and operational variations, such as temperature and traffic loading is also discussed.

2. Overview of the Guan-Du Bridge and Instrumentation

The Guandu Bridge is a steel arch bridge across the Tamsui River, Taiwan, which links two counties (Bali and Tamsui) of New Taipei City. It is a five-span continuous bridge consisting of two 44m side spans, two 143m and one 165m center spans, and its overall length is 539m. The bridge was opened for operation in October 31, 1983. The deck has four lanes for vehicles. Unique feature of the bridge design is the arch and cable system. Fig. 1 shows the photo of the bridge and the dimension of the bridge is also shown in Fig. 2.

To extract the dynamic features of the bridge in its operating condition, a short term continuous monitoring system is installed in this bridge. Twenty uni-axial accelerometers (Tokyo Sokushin AS2000) were deployed along the bridge deck (on both side of the vehicle lanes) for vibration measurement in its vertical direction. The accelerometer has frequency range of DC-250Hz, amplitude range of $\pm 2g$ and with sensitivity of 3V/g. Data communication through wireless sensing system is used to reduce the cabling issue. The wireless sensing module collected the signal from each sensor and broadcasted to PC server (about 2.0 km away) for conducting analysis. Measurements are taken from four different time period: First, from 14:00 pm of April 1st to 14:00 pm of April 2nd of 2011; Second, from 14:00 pm of August 5th to 12:00 pm of August 6th; Third, from 14:00 pm of January 17 of 2012 to 19:00 pm; Fourth, from 12:00 pm of January 19 to 16:30 pm. The

Fig. 1: Photo of Guan-Du Bridge.

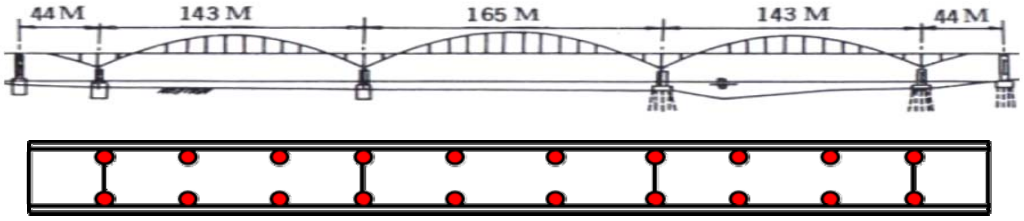

Fig. 2: Sketch of the bridge which shows the dimension as well as the locations of wireless sensing units on two sides of the bridge deck.

length of measurement is arranged to collect 1.0 min. data for every half hour with the sampling rate of 200Hz (12,000. point per minute). During the vibration measurement the outdoor temperature as well as the mean of the response variance from all sensing nodes was also calculated.

In this paper the relationship between the identified system natural frequencies and the unmeasured environmental and operational variations (traffic loading) including the ambient temperature is characterized by Nonlinear Principal Component Analysis (NLPCA).

3. Nonlinear Principal Component Analysis

The variation of the identified system modal frequencies may due to the influence of time-varying environmental and operational condition. Traffic loadings and the ambient temperature are also known to alter the measured natural frequencies and damping ratios. Therefore, in order to achieve successful novelty detection, it is necessary to develop a robust SHM system that can distinguish the effects caused by abnormality from those caused by environmental and operational variations. Peeters *et al*. [11] used a black-box model to describe the variations of eigenfrequencies as a function of temperature. The damage can be detected if the eignfrequency of the new data exceeds certain confidence intervals of the model. H. Sohn et al. employed auto-associate neural networks (AANN) to discriminate system changes on structural deterioration and damage from effects of the ambient conditions [12]. Yan *et al*. [13,14] proposed the principal component analysis (PCA) to extract the intrinsic environmental factors, and then adopted the novelty analysis to decide whether the structure is damaged or not. Sohn *et al.* [15] proposed to train an auto-associative neural network (AANN) to perform nonlinear principal component analysis (NLPCA) if the environmental effect is highly nonlinear. In this study, a NLPCA (AANN) network (with a circular node at the bottleneck), as shown in Fig. 3, which performs

the NLSSA by nonlinearly combining all the input modes into a single NLSSA mode.

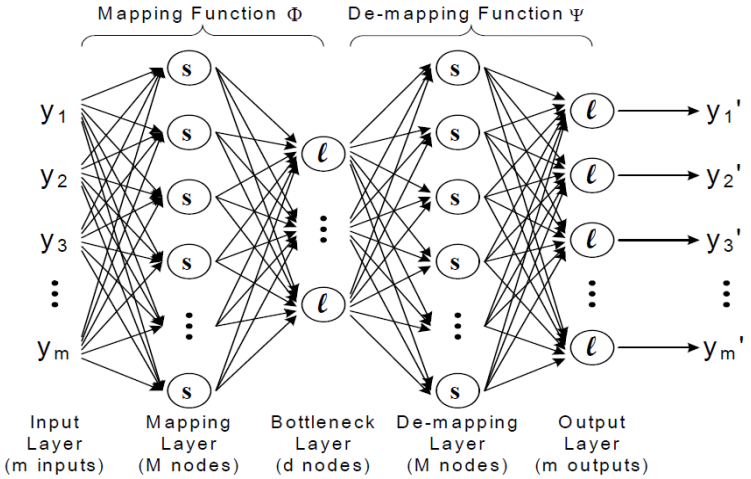

Fig 3: Auto-associate Neural Network

The input modes for AANN in this study include the identified modal frequency, variation of ambient temperature, and the Fourier amplitude induced by traffic loading. Procedures to extract the NLPCA are listed as follows:

1. Data normalization for NLPCA: A matrix is formed from the input modes, $P \in \Re^{\tilde{d} \times K}$. The component of this matrix will be used as input to auto-associate neural network. Normalization with respect to each component of the matrix, $\mathbf{P}_i$, is required to get the standardized component $\hat{\mathbf{P}}_i$. The normalization is defined as:

$$\hat{p}_{LK} = \frac{p_{LK} - \mu_L}{\mu_L} \tag{1}$$

where p_{LK} is the non-normalized value of the L-th component at time t_K and μ_L is the mean of the row vector $\mathbf{P}_i$. Each variable $\hat{\mathbf{P}}_i$; $(i = 1,2,\ldots,l)$, is a time series of length K which are the inputs to a feed-forward neural network, mapping through a bottleneck to the output $\hat{\mathbf{P}}'$.

2. Extract single mode from NLPCA: To reconstruct the single mode from AANN, the mapping from the bottleneck layer to the decoding layer needs to be done from the following equation:

$$h_k^{(\hat{p})} = \tanh((\mathbf{w}^{(\hat{p})} \cdot \hat{\mathbf{P}} + b^{(\hat{p})})_k), \quad \text{with} \quad k = 1, \ldots, M. \tag{2}$$

where $\hat{\mathbf{P}}$ is bottleneck node in NLPCA, $\mathbf{w}^{(\hat{p})}$ is a weight parameter vectors, and $b^{(d)}$ is the bias parameter. The bottleneck contains two neurons p and q confined to lie on a unit circle.

Finally, the network output is given by

$$\hat{\mathbf{P}}_i' = (\mathbf{w}^{(d)} h^{(d)} + \bar{b}^{(d)})_i \tag{3}$$

Consider the identified time-varying modal frequency and together with the ambient temperature and the Fourier amplitude of acceleration response as inputs to the AANN. After training from AANN the first NLPCA mode can be constructed.

4. Covariance-Driven Stochastic Subspace Identification

The covariance-driven stochastic subspace identification (SSI-COV) is addressing the so-called stochastic realization problem, i.e., the problem of identifying a stochastic state-space model from output-only data. Assuming a structure under consideration is being excited by un-measurable stochastic ambient forces, the discrete time stochastic state-space-model is expressed as:

$$\mathbf{x}_{k+1} = \mathbf{A}\, x_k + \mathbf{w}_k \quad \textit{and} \quad \mathbf{y}_k = \mathbf{C}\, x_k + \mathbf{v}_k \tag{4}$$

where **A** is the system matrix, **C** is the output matrix, $x_k \in \Re^{2n\times 1}$ is the state vector and $y_k \in \Re^{l\times 1}$ is the measurement vector, $\boldsymbol{w}_k$ and $\boldsymbol{v}_k$ represent the system noise and measurement noise respectively. The SSI-COV method stems from the need to solve the problem through identifying a stochastic state-space model (matrices **A** and **C**) from output-only data. The first step is to establish the data Hankel Data matrix and then form the block Toeplitz matrix by a multiplication between future and transpose of past measurements:

$$\mathbf{H} = \frac{1}{\sqrt{\mathbf{N}}}\left[\begin{array}{cccc} \mathbf{y_1} & \mathbf{y_2} & \cdots & \mathbf{y_N} \\ \mathbf{y_2} & \mathbf{y_3} & \cdots & \mathbf{y_{N+1}} \\ \cdots & \cdots & \cdots & \cdots \\ \mathbf{y_i} & \mathbf{y_{i+1}} & \cdots & \mathbf{y_{i+N-1}} \\ \hline \mathbf{y_{i+1}} & \mathbf{y_{i+2}} & \cdots & \mathbf{y_{i+N}} \\ \mathbf{y_{i+2}} & \mathbf{y_{i+3}} & \cdots & \mathbf{y_{i+N+1}} \\ \cdots & \cdots & \cdots & \cdots \\ \mathbf{y_{2i}} & \mathbf{y_{2i+1}} & \cdots & \mathbf{y_{2i+N-1}} \end{array}\right] = \left[\begin{array}{c} \mathbf{Y_p} \\ \hline \mathbf{Y_f} \end{array}\right] \quad \Rightarrow \quad \boldsymbol{T}_{1/i} = \left[\begin{array}{cccc} \boldsymbol{R}_i & \boldsymbol{R}_{i-1} & \cdots & \boldsymbol{R}_1 \\ \boldsymbol{R}_{i+1} & \boldsymbol{R}_i & \cdots & \boldsymbol{R}_2 \\ \cdots & \cdots & \cdots & \cdots \\ \boldsymbol{R}_{2i-1} & \boldsymbol{R}_{2i-2} & \cdots & \boldsymbol{R}_i \end{array}\right] = \boldsymbol{Y}_f (\boldsymbol{Y}_p)^T \tag{5}$$

where $\mathbf{Y}_p$ denotes the past measurements and $\mathbf{Y}_f$ denotes for the future measurements. The block output covariance with time lag i is defined as $\mathbf{R}_i$ and has the following factorization properties:

$$\mathbf{R}_{\mathrm{i}} = \mathrm{E}\left[\mathbf{y}_{\mathrm{k}}\ \mathbf{y}_{\mathrm{k-i}}^{\mathrm{T}}\right] = \mathbf{C}\mathbf{A}^{\mathrm{i-1}}\mathbf{G} \tag{6}$$

where **G** is the next-step state and output covariance matrix $\mathbf{G} = E[\boldsymbol{x}_{k+1}\boldsymbol{y}_k^T]$. The Toeplitz matrix can be factorized into the extended observability matrix $\mathbf{O}_i \in \Re^{li\times 2n}$ and the reversed extended stochastic controllability matrix $\boldsymbol{\Gamma}_i \in \Re^{2n\times li}$, as shown below:

$$\mathbf{T_{I/i}} = \mathbf{O}_i\boldsymbol{\Gamma}_i = \left[\begin{array}{c} \mathbf{C} \\ \mathbf{CA} \\ \cdots \\ \mathbf{CA}^{i-1} \end{array}\right]\left[\mathbf{A}^{i-1}\mathbf{G} \quad \cdots \quad \mathbf{AG} \quad \mathbf{G}\right] \tag{7}$$

Singular Value Decomposition (SVD) is used to perform the above mentioned factorization:

$$\mathbf{T_{1/i}} = \mathbf{USV}^T = \begin{pmatrix}\mathbf{U}_1 & \mathbf{U}_2\end{pmatrix}\begin{pmatrix}\mathbf{S}_1 & 0\\ 0 & 0\end{pmatrix}\begin{pmatrix}\mathbf{V}_1^T\\ \mathbf{V}_2^T\end{pmatrix} = U_1 S_1 V_1^T \tag{8}$$

where $\mathbf{U} \in \Re^{li \times li}$ and $\mathbf{V} \in \Re^{li \times li}$ are orthonormal matrices, and **S** is a diagonal matrix containing positive singular values in descending order. Comparing Eq. (7) and Eq. (8), the matrix $\mathbf{O}_i$ which contains the system matrices (**A** and **C**) can be computed by splitting the SVD in two parts:

$$\mathbf{O}_i = \mathbf{U}_1 \mathbf{S}_1^{1/2} \quad and \quad \mathbf{\Gamma}_i = \mathbf{S}_1^{1/2}\mathbf{V}_1^T \tag{9}$$

From $\mathbf{O}_i$ matrix, the system matrices (**A** and **C**) can be obtained easily. In MATLAB notation, the C matrix is just the first block of $\mathbf{O}_i$, i.e. $C = O_i(1:l,:)$. Then system matrix **A** can be computed by exploiting the shift structure of the extended observability matrix $\mathbf{O}_i$:

$$\begin{bmatrix}\mathbf{CA}\\ \mathbf{CA}^2\\ \dots\\ \mathbf{CA}^i\end{bmatrix} = \begin{bmatrix}\mathbf{C}\\ \mathbf{CA}\\ \dots\\ \mathbf{CA}^{i-1}\end{bmatrix}\mathbf{A} \qquad \text{and} \quad \mathbf{A} = \mathbf{O}_1(1:l(i-1),:)^{\lambda^*}\mathbf{O}_i(l+1:li,:) \tag{10}$$

where $(\cdot)^{\lambda}$ denotes pseudo-inverse. The system matrix **A** is extracted by taking advantage of the shift structure of matrix $\mathbf{O}_i$, and the pseudo-inverse of $\mathbf{O}_i$ is to determine the system matrix **A** in a least square sense. The modal frequencies and effective damping ratios can be computed by conducting eigenvalue decomposition of the system matrix **A**, and the corresponding eigenvectors multiplied by the output matrix **C** are used to observe mode shapes.

The actual implementation of SSI-COV consists of estimating the covariance R, computing the SVD of $T_{1/i}$, truncate the SVD to the model order n, estimating O_i and Γ_i by splitting the SVD in two parts and finally estimating A, C, G from O_i and Γ_i. However, to obtain a good model for modal order analysis applications, it is probably a better idea to construct a stabilization diagram, by indentifying a whole set of models with different order.

5. Recursive Stochastic Subspace Identification

The above-mentioned SSI techniques process measured data in one batch hence cannot be used for on-line health monitoring and damage detection. Therefore, for on-line tracking of time-varying structural modal parameters a recursive subspace method needs to be developed. Instead of arranging the block covariance in the form of so-called Toeplitz matrix, the form of a Hankel Covariance matrix must be adopted which can be constructed by arranging the output measurement data vectors as

follows:

$$\mathrm{y}_k^+ \equiv \begin{bmatrix} \mathrm{y}_{k-i+1} \\ \mathrm{y}_{k-i+2} \\ \cdots \\ \mathrm{y}_k \end{bmatrix}, \quad \mathrm{y}_k^{-T} \equiv \begin{bmatrix} \mathrm{y}_{k-i}^T & \mathrm{y}_{k-i-1}^T & \cdots & \mathrm{y}_{k-2i+1}^T \end{bmatrix} \tag{11}$$

where $\boldsymbol{y}_k \in \Re^{l\times 1}$ is the output measurement vector. $\boldsymbol{y}_k^+ \in \Re^{il\times 1}$ and $\boldsymbol{y}_k^{-T} \in \Re^{1\times il}$. l is the number of sensors and i is number of block rows. A Hankel covariance matrix, $\mathbf{H}_N^{COV}$, is defined:

$$\mathbf{H}_N^{cov} = E\left[\mathrm{y}_k^+ \mathrm{y}_k^{-T}\right] = \frac{1}{\tilde{p}} \sum_{k=2i}^{N} \mathrm{y}_k^+ \mathrm{y}_k^{-T} \tag{12}$$

$$= \begin{bmatrix} \boldsymbol{y}_{i+1} & \boldsymbol{y}_{i+2} & \cdots & \boldsymbol{y}_{N-i+1} \\ \boldsymbol{y}_{i+2} & \boldsymbol{y}_{i+3} & \cdots & \boldsymbol{y}_{N-i+2} \\ \vdots & \vdots & & \vdots \\ \boldsymbol{y}_{2i} & \boldsymbol{y}_{2i+1} & \cdots & \boldsymbol{y}_N \end{bmatrix} \begin{bmatrix} \boldsymbol{y}_i^T & \boldsymbol{y}_{i-1}^T & \cdots & \boldsymbol{y}_1^T \\ \boldsymbol{y}_{i+1}^T & \boldsymbol{y}_i^T & \cdots & \boldsymbol{y}_2^T \\ \vdots & \vdots & & \vdots \\ \boldsymbol{y}_{N-i}^T & \boldsymbol{y}_{N-i-1}^T & \cdots & \boldsymbol{y}_{N-2i+1}^T \end{bmatrix} = \mathbf{Y}_k^+ \mathbf{Y}_k^{-T}$$

where k is ranging over the entire set of available data, and the order of the Hankel Covariance matrix is "i" with data length N. The need of a recursive fashion to update SVD is required. A new approach called Projection Approximation Subspace Tracking (PAST) was initially developed by Bin Yang [16], which takes the advantage of a mathematical lemma to find the required column subspace as an unconstrained optimization problem. Later the algorithm is modified to its Extended Instrumental Variable version (EIV-PAST) by Gustafsson [17], which is a suitable algorithm for the structure of SSI-COV.

To derive the RSSI, the Extended Instrument Variable technique is used. The cost function to be minimized can be replaced by its corresponding EIV formulation:

$$\overline{V}\left[\mathbf{W}(t)\right] = \left\| \sum_{k=1}^{t} \mathrm{z}(k)\xi^H(k) - \mathbf{W}(t) \sum_{k=1}^{t} \mathrm{h}(k)\xi^H(k) \right\|_F^2 = \left\| \mathbf{C}_{z\xi}(t) - \mathbf{W}(t)\mathbf{C}_{h\xi}(t) \right\|_F^2 \tag{13}$$

where $\boldsymbol{h}(k) = \mathbf{W}^H(k-1)\boldsymbol{z}(k)$ and the subscript $_F$ denotes the Frobenius norm defined as $\sqrt{tr\left(\boldsymbol{\sigma}\boldsymbol{\sigma}^H\right)}$. The least square solution of Eq.13 is readily found to be:

$$\mathbf{W}(t) = \overline{\mathbf{U}}'_{EIV}(t) = \mathbf{C}_{z\xi}(t)\mathbf{C}_{h\xi}^T(t)\left[\mathbf{C}_{h\xi}(t)\mathbf{C}_{h\xi}^T(t)\right]^{-1} \tag{14}$$

where $\mathbf{C}_{z\xi}(t) = \sum_{k=1}^{t} \mathrm{z}(k)\xi^H(k) = \mathbf{C}_{z\xi}(t-1) + \mathrm{z}(t)\xi^H(t)$ and

$$\mathbf{C}_{h\xi}(t) = \sum_{k=1}^{t} \mathrm{h}(k)\xi^H(k) = \mathbf{C}_{h\xi}(t-1) + \mathrm{h}(t)\xi^H(t)$$

W is a matrix with suitable dimension and has orthogonal columns containing any "r" distinct eigenvectors and the RLS algorithm can be easily derived for updating **W**(t). By substituting the random vector $\boldsymbol{z}(t)$ and the instrument $\boldsymbol{\xi}(t)$ by the corresponding data vector in Eq.11, the objective function of EIV-PAST to be minimized will

become:

$$\overline{V}[\mathbf{W}(t)] = \left\| \sum_{k=t-L+2i}^{t} \boldsymbol{y}_k^+ \boldsymbol{y}_k^{-T} - \mathbf{W}(t) \sum_{k=t-L+2i}^{t} \overline{\boldsymbol{h}}(k) \boldsymbol{y}_k^{-T} \right\|_F^2 = \left\| \mathbf{H}_t^{\text{cov}} - \mathbf{W}(t) \overline{\mathbf{H}}_t^{\text{cov}} \right\|_F^2 \tag{15}$$

Similar to Eq.14 the least square solution of Eq.15 can be obtained as follows:

$$\mathbf{W}(t) = \mathbf{U}_1(t) = \left(\mathbf{H}_t^{\text{cov}} \overline{\mathbf{H}}_t^{\text{cov}\,T} \right) \left(\overline{\mathbf{H}}_t^{\text{cov}} \overline{\mathbf{H}}_t^{\text{cov}\,T} \right)^{-1} \tag{16}$$

Therefore, the column subspace **U** can also be obtained from the Eigen-Decomposition (ED) of the Hankel Covariance matrix multiplied by its transpose (the covariance of the Hankel Covariance matrix).

Application of EIV-PAST to RSSI-COV In SSI-COV algorithm the SVD of a Hankel Covariance matrix is defined as:

$$\mathbf{H}^{\text{cov}} = \mathbf{U}\mathbf{S}\mathbf{V}^T = \begin{pmatrix} \mathbf{U}_1 & \mathbf{U}_2 \end{pmatrix} \begin{pmatrix} \mathbf{S}_1 & 0 \\ 0 & 0 \end{pmatrix} \begin{pmatrix} \mathbf{V}_1^T \\ \mathbf{V}_2^T \end{pmatrix} \tag{17}$$

where **U** and **V** are orthonormal matrices, **S** is a diagonal matrix containing the singular values. Since the Hankel Covariance matrix multiplied by its transpose can also be expressed as:

$$\mathbf{H}^{\text{cov}} \mathbf{H}^{\text{cov}^T} = \mathbf{U}\mathbf{S}\mathbf{V}^T \mathbf{V}\mathbf{S}^T \mathbf{U}^T = \mathbf{U}\left(\mathbf{S}\mathbf{S}^T\right)\mathbf{U}^T = \mathbf{U}\left(\mathbf{S}\mathbf{S}^T\right)\mathbf{U}^{-1} \tag{18}$$

From the procedure of SSI-COV the desired system observability matrix $\mathbf{O}_i$ can be obtained by extracting the column subspace $\mathbf{U}_1$ from Hankel Covariance matrix using SVD. However, after solving Eq.17 by least square, the obtained dominant eigenvector $\mathbf{W}(t) = \overline{\mathbf{U}}'_{IV}(t)$ is actually the dominant eigenvectors of the Hankel ovariance matrix instead of the desired column subspace. This latter must be computed via ED of the "Covariance matrix of the Hankel Covariance matrix" as shown in Eq.17. Hence, the Extended Instrumental Variable Recursive Least Square (EIV-RLS) algorithm can be applied to solve the EIV-PAST problem, which fulfills the SVD-updating requirement of RSSI-COV to track the time-varying subspace $\mathbf{U}_1$(t).

To develop the adaptive Hankel covariance matrix for RSSI-COV, a new incoming data point *N+1* will be added to the exsisting Hankel covariance matrix and converted into a new rank-one matrix. The sliding window technique will be used to formulate the adaptive Hankel matrix for RSSI-COV, although this requires more computations, but it offers a faster tracking response to sudden signal changes [16]. The sliding window technique requires 2 steps calculation for each incoming new data: First, the oldest data is removed from the window (down-dating); and second, a new data is incorporated (up-dating). Let the window length remains to be L, and then the adaptive Hankel matrix is expressed as:

$$\mathbf{H}_{N+1}^{\text{cov}} = \mathbf{H}_N^{\text{cov}} + \boldsymbol{y}_{N+1}^+ \left(\boldsymbol{y}_{N+1}^-\right)^T - \boldsymbol{y}_{N-L+2i}^+ \left(\boldsymbol{y}_{N-L+2i}^-\right)^T \tag{19}$$

The use of moving window technique implies the EIV-RLS algorithm has to be done twice to complete the subspace updating: after adding the new incoming data (up-dating) the oldest data from the moving window must be discarded (down-dating). Once the time-varying column subspace $\mathbf{U}_1(t)$ is estimated, the system information can then be extracted.

6. Monitoring Results of the Guan-Du Bridge

The proposed RSSI-COV method that incorporated with NLPCA is applied to the field data collected from the Guan-Du Bridge to investigate its ability to detect abnormality in the presence of environmental and operational variations. Before conduct the RSSI-COV to extract the system natural frequencies, first, the offline SSI-COV is applied to identify the dominant frequencies of the bridge as well as the mode shapes of the bridge.

Stabilization Diagram and system identification As the system order is often unknown, a common practice on operational modal analysis is to calculate the modal parameters for increasing

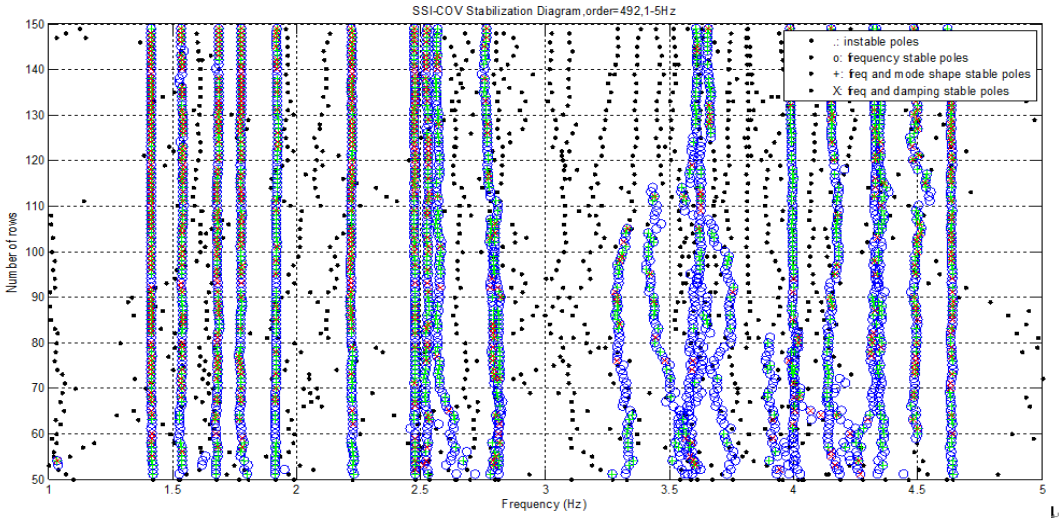

Fig. 4 Stability diagram from SSI-COV with system order of 492.

Table 1: Estimated natural frequencies and damping ratios

Mode	1	2	3	4	5	6	7	8	9	10	11
Freq. (Hz)	1.39	1.56	1.65	1.78	1.92	2.23	2.47	2.52	2.57	2.77	2.89
Damping Ratio (%)	1.3	1.3	1.1	1.0	0.8	1.0	0.1	0.7	5.6	0.6	
Note		Symmetric vs. Anti-symmetric modes									
			Symmetric vs. Anti-symmetric modes								
				Symmetric vs. Anti-symmetric modes							

model order “n”. If n is higher than the true system order, the noise is modeled, but the mathematical poles that raise in this way are different from for different model orders if the noise is purely white. So the true physical system poles can be detected by comparing the modal parameters for different modal orders. The detection can be performed in a stabilization diagram. In this study a total of 20 sensors are used. Since

the original data sampling rate is 200 Hz, to reduce the computation time as well as the dimension of the Hankel matrix, down-sampling to 50 Hz by using the Butterworth IIR filter of order 10 is used. The dimension of Toeplitz matrix is (*3000×3000*) in which *i=150* and *j=2701*. Fig. 4 shows the stabilization diagram obtained from SSI-OV method. For such a bridge, its dominant frequencies of interest lie in the range of 0-5 Hz. The estimated natural frequencies and damping ratios by the proposed method and the SSI technique are given in Table 1. A typical stabilization diagram is implemented by comparing the poles obtained between two consecutive matrix order from lowest to highest, then apply stabilization criteria to modal frequencies, damping ratios and mode shapes, to discriminate if a pole is stable or not. The chosen stability criteria are referenced from [9] and are defined as follows:

$$\begin{aligned} &\text{Modal frequency: } \left(\left(f^{(i+1)}-f^{(i)}\right)/f^{(1)}\right)\times 100\% \le 1\% \\ &\text{Modal damping ratio: } \left(\left(\zeta^{(i+1)}-\zeta^{(i)}\right)/\zeta^{(i)}\right)\times 100\% \le 5\% \\ &\text{Mode shape: } \left(1-MAC(i,i+1)\right)\times 100\% \le 3\% \end{aligned} \tag{20}$$

where i is the number of block rows of the Hankel matrix, which determines the Toeplitz or projection matrix order, and *MAC* is the Modal Assurance Criterion, which is defined as the squared correlation between two mode shape vectors:

$$MAC(i,i+1)=\frac{(\boldsymbol{v}^{(i+1)^H}\boldsymbol{v}^{(i)})^2}{(\boldsymbol{v}^{(i+1)^H}\boldsymbol{v}^{(i+1)})(\boldsymbol{v}^{(i)^H}\boldsymbol{v}^{(i)})} \tag{21}$$

where the subscript ^{H} denotes Hermitian transpose, $\boldsymbol{v}$ is the given mode shape vector, and *MAC* is a scalar between zero and unity. Generally, the system poles are more stable in terms of its modal frequency as the matrix order is increased, followed by mode shape, and damping ratio is the most unstable quantity. Fig. 5 shows the identified mode shapes (for frequencies lower than 3.0 Hz). It is important to point out that both symmetric and anti-symmetric modes can be identified. As shown in Fig. 6, the identified mode shapes for f=1.56 Hz versus f=2.57 Hz, f=1.65 Hz versus f=2.77 Hz, and f=1.78 Hz versus f=2.89 Hz are symmetric versus anti-symmetric mode, respectively.

Quantification of Vibration Amplitude Since the response measurement of the bridge is mainly caused by traffic-induced vibration, it is necessary to quantify the bridge vibration amplitude so as to achieve successful novelty detection. To quantify the bridge vibration amplitude during a specific time window caused by environmental and operational variation, a systematic way of extracting

vibration amplitude needs to be established. Consider a specific time window of analysis in which the Fourier amplitude spectrum from each measurement is calculated. The frequency band of the spectrum needs to cover all dominant frequencies that were identified from SSI-COV. It is defined:

$$\mathbf{F} = [\{\hat{\boldsymbol{f}}_1\}\ \{\hat{\boldsymbol{f}}_2\}\ \cdots\ \{\hat{\boldsymbol{f}}_n\}] \tag{22}$$

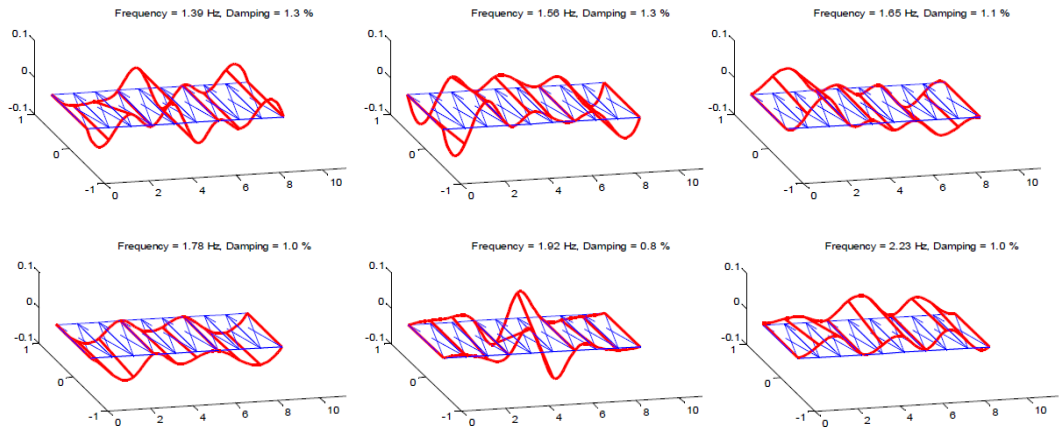

Fig. 5: Identified the first six fundamental mode shapes of Guan-Du Bridge.

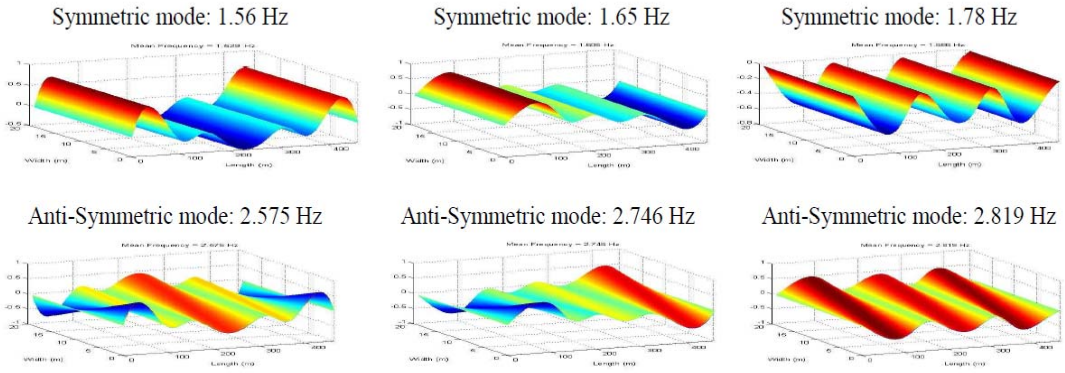

Fig. 6: Plot the identified symmetric and anti-symmetric modes of Guan-Du Bridge.

where n is the number of sensors and $\{\hat{\boldsymbol{f}}_i\}$ is a vector which listed all the Fourier amplitude spectrum from response measurement at sensor node "i". Principal component analysis (PCA) is used through singular value decomposition to extract the principal component of the response Fourier amplitude:

$$\mathbf{F} = [\{\hat{\boldsymbol{f}}_1\} \ \{\hat{\boldsymbol{f}}_2\} \ \cdots \ \{\hat{\boldsymbol{f}}_n\}] = \mathbf{U}\,\mathbf{S}\,\mathbf{V}^T \tag{23}$$

The first principal component, is a function of frequency, can be extracted. The amplitude from the 1st PCA can be used as the quantification of the vibration amplitude.

Application of RSSI-COV method Application of the proposed recursive stochastic subspace identification scheme to the response measurement of Guan-Du Bridge, the time-varying system natural frequencies can be identified. The time window for recursive identification is 45 sec. and moving with 5.0 sec interval. The identification scheme is shown in Fig. 7, and the related model parameters for RSSI are also indicated in this flowchart. It is important to point out that data pre-processing is important in order to have a better results of identification and can reduce the computation time. Fig. 8 only plots the identified time-varying system natural frequencies at 1.56 Hz (symmetric mode) and 2.57 Hz (anti-symmetric mode) from five different time period of measurement. The two identified frequencies in this

figure will have the same mode shape with MAC higher than 60%. Other system natural frequencies can also have the same results. It is observed that the time-variation of the identified system natural frequencies do exist.

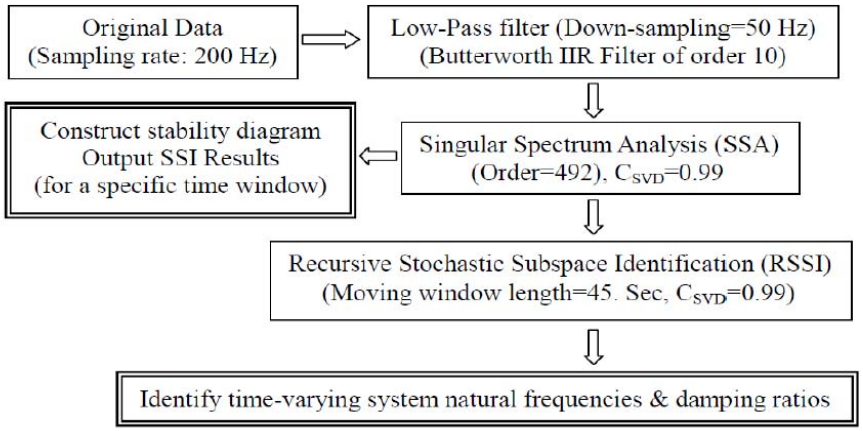

Fig. 7: Flowchart of data analysis and identification procedures.

Nonlinear Principal Component Analysis To distinguish the change of system natural frequency caused by abnormality from those caused by environmental and operational variation the nonlinear principal component analysis is applied. Based on the above mentioned AANN method, the relationship (nonlinear principal component) among the identified system natural frequency (f=1.554 Hz), ambient temperature and Fourier amplitude of response at specify system frequency is investigated. Fig. 9a plots the 3-D relationship between the normalized three physical parameters. The extracting principal component from the data is also shown in this figure. To plot the 2-D relationship Fig. 9b shows the relationship between the normalized system natural frequency and the ambient temperature. It is observed that the system natural frequency decreases with the increasing ambient temperature. Same analysis can also be applied to different system natural frequency.

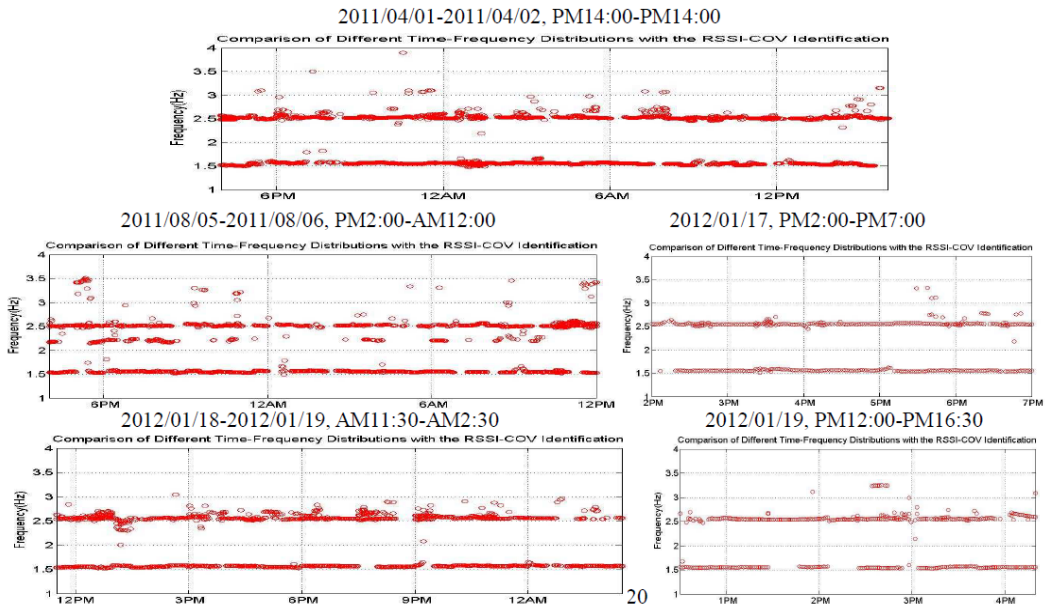

Fig. 8: Plot the time-varying bridge natural frequencies (f=1.56 Hz and f=2.575 Hz) from five different time period of monitoring.

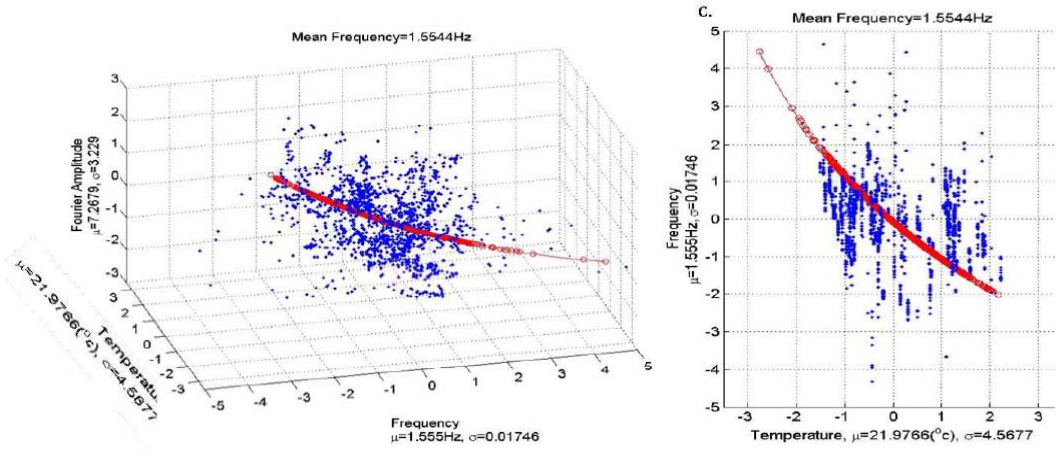

Fig. 9: (a) 3-D plot on the relationship among bridge vibration frequency (f=1.55 Hz), ambient temperature and the vibration amplitude. The nonlinear principal component is also shown, (b) 2-D plot on the relationship between Fourier amplitude and temperature.

7. Conclusions

This paper presented the on-line system parameter estimation technique from the response measurements through Recursive Covariance-driven Stochastic Subspace identification (RSSI-COV) approach. To avoid excessive time-consumption in Singular Value Decomposition, Extended Instrumental Variable Projection Approximation Subspace Tracking algorithm (EIV-PAST) is used for this study. With the proposed method a bridge structure monitoring system is developed. Through the output-only response measurement a Stochastic Subspace Identification (SSI) is carried out to extract the dynamic characteristics of the bridge under its operating condition. To distinguish the abnormality of the identified system natural frequencies from those caused by environmental and operational variation, the time-varying modal parameters using recursive SSI-COV algorithm was developed. The accuracy and robustness offered by RSSI-COV can extract the key feature directly from the response measurement to obtain the evidences of system changes and provides a very stable modal frequency tracking. In this study, the nonlinear principal component analysis is employed to extract the nonlinear relationship between system natural frequencies, ambient temperature and amplitude of external traffic loadings. Through this study the following conclusions are drawn:

1. Pre-processing of the measurement can provide accurate result from using SSI, and can also speed up the calculation. For recursive stochastic subspace identification, it is necessary to develop a new filtering algorithm to down-sampling the data.
2. Application of RSSI-COV to identify the system dynamic characteristics, it is important to select suitable model parameters for stochastic subspace identification. These parameters include: the length of moving time window, the number of order for Hankel matrix, and Percentage of Singular Values (C_{SVD}) needs to be considered
3. Incorporated with ANN the Nonlinear PCA technique is employed to extract the

nonlinear relationship among the identified system natural frequency, ambient temperature and the vibration amplitude of the measurements.

References

[1] Van Overschee P. and De Moor B. *Subspace Identification for Linear Systems: Theory - Implementation – Applications*. Kluwer Academic Publishers, Dordrecht, The Netherlands, 1996.

[2] Bart Peeters. *System Identification and Damage Detection in Civil Engineering*. Ph.D. Dissertation, Katholieke Universiteit, Leuven, December 2000.

[3] Bart Peeters and Guido De Roeck, "Reference-based stochastic subspace identification for output-only modal analysis," *Mechanical Systems and Signal Processing* 13(6) 1999, 855-878.

[4] Peeters, B., De Roeck, G., "Stochastic system identification for operational modal analysis: a review," J. Dyn. Syst. Meas. Control 123, 2001, 659-666.

[5] Bassville,M., Benveniste, A., Goursat, M. and Mevel, L. "In-flight vibration monitoring of aeronautical structures," IEEE Control System Magazine, October 2007, 27-41.

[6] Weng, J.H., Loh, C.H., Lynch, J.P., Lu, K.C., Linn, P.Y., Wang, Y., "Output-Only Modal Identification of a Cable-Stayed Bridge Using Wireless Monitoring Systems," J. of Eng. Structure, 30 (2), 2008, 1802-1830.

[7] Boonyapinyo, V. and Janesupasaeree, T. "Data-driven stochastic subspace identification of flutter derivatives of bridge decks," J. wind Eng. Ind. Aerodyn. 98, 2010, 784-799.

[8] De Cock K., Mercère G., De Moor B. "*Recursive subspace identification for in-flight modal analysis of airplanes*". Proceedings of the International Conference on Noise and Vibration Engineering (ISMA 2006), Leuven, Belgium, Sept. 2006, pp. 1563-1577.

[9] Loh, C.H.; Weng, J.H.; Liu, Y.C.; Lin, P.Y. and Huang, S.K. "*Structural damage diagnosis based on on-line recursive stochastic subspace identification*". Smart Mater. Struct. 20 (2011) 055004.

[10] Goethals, I.; Mevel, L.; Benveniste, A.; and De Moor, B. "*Recursive output only subspace identification for in-flight flutter monitoring*". Proc. of the 22nd International Modal Analysis Conference, Dearborn, Michigan, 2004.

[11] Peeters B., and De Roeck G. "One-year monitoring of the Z24-Bridge: environmental effects versus damage events." Earthquake Eng. and Structural Dynamics, 30, 2001, 149-171.

[12] Sohn H., Dzwonczyk M., Straser E.G., Kiremidjian A.S., Law K.H., Meng T. "An experimental study of temperature effect on modal parameters of the Alamosa Canyon Bridge." *Earthquake Engineering and Structural Dynamics*, 28, 1999, 879–897.

[13] Yan A.M., Kerschen G., De Boe P., Golinval J.C. "Structural damage diagnosis under changing environmental conditions—Part I: A linear analysis." *Mech. Sys. and Signal Proc.*, 19, 2005, 847-864.

[14] Yan A.M., Kerschen G., De Boe P., Golinval J.C. (2005) "Structural damage diagnosis under changing environmental conditions—Part II: local PCA for non-linear cases." *Mechanical Systems and Signal Processing*, 19, 865-880.

[15] Sohn H., Worden K., Farrar C.F. "Novelty detection under changing environmental conditions." *SPIE's 8th Annual Int. Symposium on Smart Structures and Materials*, Newport Beach, CA.2001.

[16] Yang, Bin. "*Projection Approximation Subspace Tracking*". IEEE transactions on signal processing, Vol. 43, No. I, January 1995.

[17] Gustafsson T. "*Instrumental Variable Subspace Tracking Using Projection Approximation*". IEEE transactions on signal processing, Vol. 46, No. 3, March 1998.

[18] Mercère, G., Lecoeuche, S., and Lovera, M. "*Recursive subspace identification based on instrumental variable unconstrained quadratic optimization*". International J. of Adaptive Control and Signal Processing, 18, 771-797, 2004.

[19] Söderström, Torsten and Stoica, Petre. "*System identification*". Prentice-Hall International, 1989.

Part 2:

Develop On-Line Damage Detection Methods of Bridge Under Abnormal Conditions

ABSTRACT

The objective of this paper is to discuss two different approaches on structural damage detection: one is the vibration-based damage detection and the other is the model-based damage detection. The vibration-based damage detection method is based on the extracted sub-space or null-space from the singular value decomposition (SVD) of analytic matrix formed from data Hankel matrix. Damage detection algorithm is then developed by considering the orthonormality between the subspace and null-space. To form the analytic matrix three different algorithms can be used: from the trajectory matrix in Singular Spectrum Analysis (SSA), from Toeplitz matrix in SSI-COV, or from QR decomposition of data Hankel matrix in SSI-DATA. The model-based damage detection is using the AR-ARX model to identify the model coefficients from which the damage sensitivity factor can be generated. Discussion among these damage detection methods was made through the response data collected from the shaking table test of a 6-stry steel frame with different damage scenarios and the scouring test of bridge model in hydraulic lab during scouring process.

1. INTRODUCTION

Continuous vibration monitoring provides a valuable tool to complement other nondestructive evaluation methods. It directly addresses the performance of the structural condition under service loading. Damage identification based upon changes in dynamic response is one of the few methods that monitoring changes in the

structure on a global basis. The premise of vibration-based damage detection approach is that the damages will significantly alter the dynamic response, due to changes in structural dynamic characteristics or the structural boundary conditions. To achieve this damage detection goal, techniques on structural health monitoring need to be developed. The structural health monitoring process involves the monitoring of a structure over time, the periodically collection of response measurement from an array of sensors, the extraction of damage sensitive features through analyzing the data, and determine the current state of the health. Early damage detection and eventual estimation of damage is an important problem, since it forms the basis of any decision for structural repair and/or part replacement.

There are several damage detection methods without using input information. The results include different experimental techniques, methodologies and signal processing methods, as indicated by Doebling *et al*. in 1996 and Staszewski in 1996 [1,2]. Most damage detection methods use a relationship between a structure condition and a diagnostic symptom indicating damage. The emergency of damage can be indicated by a change of these symptoms. However, due to the complexity of engineering structures, it is difficult to observe small changes of symptoms which can lead to early damage detection. Therefore, different signal processing methods are used to obtain features for damage symptoms. It appears that in practice that signal processing is a crucial element in the implementation and operation of any damage detection system.

Considering vibration-based signal processing and feature extraction, singular value decomposition (SVD) has been widely used in many different system identification and damage detection methods. Many publications start to apply SVD to detect structural damage. Ruotolo and Surace [3] investigated SVD for damage detection by comparing current sensor data to a subspace spanned by measurements taken from the healthy structure with varying operational and environmental conditions. Yan and Golinval performed SVD to obtain characteristic subspace from measurements [4]. It was demonstrated that the structural features are mainly located in the active subspace, which is orthonormal to the null subspace. If damage occurs the orthonormality relation between two subspaces will be broken. In relating to SVD singular spectrum analysis (SSA) has been used as an alternative to traditional digital filtering method. SSA procedure mainly involves two stages: decomposition and reconstruction. It takes singular value decomposition of Hankel matrix embedded by analyzed time series and decomposes it into several simple, independent and identifiable components. It is a novel technique of time series analysis and signal feature extraction. The development of SSA is associated with publication of several papers by Broomhead et al. [5,6] and Bosso et al. [7]. The basic capabilities of SSA include finding trend, extracting periodic component, smoothing time series and de-noising of time series which can be used for damage detection.

Time-series analysis based on the use of autoregressive (AR) model has also

been extensively used in the SHM process as a feature extraction and damage detection technique by Sohn & Farrar [8]. This technique is typically applied to experimentally measured time-series data where future data values are predicted from past values. The residual errors have had considerable applications as damage-sensitive features. Furthermore, in addition to the widely used residual errors, the estimated AR coefficients are also directly used as damage-sensitive features. The AR model coefficients are used to define the feature vector which serves as the diagnostic tool for damage identification had been developed by Nair, et al. [9] and Nair and Kiremidjian [10]. This approach intends to extract features capable of being sensitive to the effects caused by damage and insensitive to the effects due to operational and environmental variations.

The application of system identification to vibrating structures yields a research domain in civil engineering, known as experimental modal analysis (EMA). In this paper two different types of system identification and feature extraction techniques are discussed for generating the damage indices for damage detection. The first one is the subspace-based damage detection by using singular value decomposition of data Hankel matrix or analysis matrix (*i.e.* using null-space and subspace-based damage detection); the second one is using the time-dependent ARX model and generate damage sensitive features for damage detection (*i.e.* using autoregressive (AR) model coefficients or using residual error of two-tier AR-ARX model). Methodologies from these two techniques, which include five different definitions of damage indices, are introduced and briefly summarized. The performances of these five damage indices are investigated through comparative study of using response measurement from scenario damage of a steel frame subject to white noise excitation and the bridge scouring test in large hydraulic laboratory.

2. REVISITS TO DAMAGE IDENTIFICATION METHODS

2.1. Null Subspace-based Damage Detection

Considering two matrices, $\mathbf{X_0}$ and $\mathbf{X}$ refer to the analysis matrices represented by the data from health (reference) system and monitor (target) system, respectively. The results from singular value decomposition of these two matrices are expressed as:

$$\mathbf{X}_0 = [\mathbf{U}_{s0} \quad \mathbf{U}_{n0}] \begin{bmatrix} \mathbf{S}_{s0} & \mathbf{0} \\ \mathbf{0} & \mathbf{S}_{n0} \end{bmatrix} [\mathbf{V}_{s0} \quad \mathbf{V}_{n0}]^{\mathrm{T}} \approx \mathbf{U}_{s0}\mathbf{S}_{s0}\mathbf{V}_{s0}^{*} \tag{1}$$

$$\mathbf{X} = [\mathbf{U}_{s} \quad \mathbf{U}_{n}] \begin{bmatrix} \mathbf{S}_{s} & \mathbf{0} \\ \mathbf{0} & \mathbf{S}_{n} \end{bmatrix} [\mathbf{V}_{s} \quad \mathbf{V}_{n}]^{\mathrm{T}} \approx \mathbf{U}_{s}\mathbf{S}_{s}\mathbf{V}_{s}^{*} \tag{2}$$

where $\mathbf{U_s}$ (or $\mathbf{U_{so}}$) and $\mathbf{V_s}$ (or $\mathbf{V_{so}}$) are subspaces of matrix $\mathbf{X}$ spanned by left singular vectors and right singular vectors corresponding to non-zero singular values respectively; $\mathbf{U_n}$ (or $\mathbf{U_{no}}$) and $\mathbf{V_n}$ (or $\mathbf{V_{no}}$) are null-spaces of matrix $\mathbf{X}$ spanned by left

singular vectors and right singular vectors corresponding to zero singular values respectively. The subspaces and null-spaces of matrices $\mathbf{X_0}$ and $\mathbf{X}$ satisfy the orthogonal property. If the target system is undamaged, the subspace of the matrix $\mathbf{X}$ will be approximately equal to the subspace of the matrix $\mathbf{X_0}$ of the reference system. Therefore, one approach to detect the damage between the target and the reference systems is by checking the orthogonal property between the null-space of the health (reference) system and the sub-space of the healthy system:

$$\mathbf{U_s U_{n0}^T = 0} \quad \text{or} \quad \mathbf{V_s V_{n0}^T = 0} \quad \text{if monitor system is undamaged}$$

$$\mathbf{U_s U_{n0}^T \neq 0} \quad \text{or} \quad \mathbf{V_s V_{n0}^T \neq 0} \quad \text{if monitor system is damage}$$

For computation simplicity, consider only the subspace and null-space spanned by left singular vector. The damaged indicator, DI_n, based on the null-space of the matrix $\mathbf{X_0}$ can be defined as the absolute mean value of the matrix evaluated from subspace and null-space:

$$DI_n = mean\{\left|\mathbf{U_s U_{n0}^T}\right|\} \tag{3}$$

where $mean\{\}$ evaluates the mean value of all elements of matrix in $\{\}$ and $|\bullet|$ makes all elements of matrix positive. The value of DI_n ranges from 0 to 1.

Different from the damage index shown in Eq. (3), the subspaces of matrix $\mathbf{x_0}$ and **x also** satisfied the following orthogonal properties:

$$\sum_{i=1}^{K}(\mathbf{x_{0i}^T x_{0i}} - \mathbf{x_{0i}^T U_{s0} U_{s0}^T x_{0i}}) \approx 0 \quad \text{if} \ \mathbf{S_{n0} \approx 0} \tag{4a}$$

$$\sum_{i=1}^{K}(\mathbf{x_i^T x_i} - \mathbf{x_i^T U_s U_s^T x_i}) \approx 0 \quad \text{if} \ \mathbf{S_n \approx 0} \tag{4b}$$

Using Eq. (4), the difference between two subspaces can be used to evaluate the projection of the column vector of the matrix $\mathbf{X}$ (target) on the subspace of the matrix $\mathbf{X_0}$ (reference state) as:

$$\sum_{i=1}^{K}(\mathbf{x_i^T x_i} - \mathbf{x_i^T U_{s0} U_{s0}^T x_i}) \approx 0 \quad \text{if monitor system is undamaged} \tag{5a}$$

$$\sum_{i=1}^{K}(\mathbf{x_i^T x_i} - \mathbf{x_i^T U_{s0} U_{s0}^T x_i}) \neq 0 \quad \text{if monitor system is damaged} \tag{5b}$$

After normalization with respect to the norm of matrix $\mathbf{X}$, the damage indicator DI_s can be defined as:

$$DI_s = \frac{\sum_{i=1}^{K}(\mathbf{x_i^T x_i} - \mathbf{x_i^T U_{s0} U_{s0}^T x_i})}{\sum_{i=1}^{K}\mathbf{x_i^T x_i}} \tag{6}$$

The denominator of Eq.(6) is used to normalize the damage index DI_s so as to have DI_s in the range between 0 and 1.

To create an analysis matrix for SVD to develop damage index, three different

definitions on the analysis matrix can be defined. First one, consider the process on Data-driven Stochastic Subspace Identification algorithm (SSI-DATA). The first step of SSI-DATA is the LQ decomposition of the data Hankel matrix, as shown:

$$\mathbf{Y} = \begin{bmatrix} \mathbf{y[1]} & \mathbf{y[2]} & \cdots & \mathbf{y[K]} \\ \mathbf{y[2]} & \mathbf{y[3]} & \cdots & \mathbf{y[K+1]} \\ \vdots & \vdots & \ddots & \vdots \\ \mathbf{y[L]} & \mathbf{y[L+1]} & \cdots & \mathbf{y[N]} \end{bmatrix} = \begin{bmatrix} \mathbf{Y_p} \\ \hline \mathbf{Y_f} \end{bmatrix} = \begin{bmatrix} \mathbf{L_{11}} & \mathbf{0} \\ \mathbf{L_{21}} & \mathbf{L_{22}} \end{bmatrix} \begin{bmatrix} \mathbf{Q_{11}^T} \\ \mathbf{Q_{21}^T} \end{bmatrix} \tag{7}$$

and then takes the singular value decomposition of the element matrix $\mathbf{L_{21}}$ of lower triangular matrix to obtain the observability matrix **O**. The analysis matrix **X** for damage detection can be defined as:

$$\mathbf{X} = \mathbf{L_{21}} \mathbf{L_{21}^T} \tag{8}$$

To identify a suitable system order for SSI-DATA so as to separate the significant singular values from the noise (or null-space), the system model order "n" can be determined from the selected number of singular spectrum in conducting the SV based on the proposed C_{SVD} value which is defined as:

$$C_{SVD} = \sum_{i=1}^{n} s_i \Big/ \sum_{i=1}^{N} s_i \tag{9}$$

where s_i is the value of singular spectrum and N is the total number of singular values along the diagonal of matrix [S] in SVD and with ($n<N$).

The second one to define the analysis matrix for defining the damage index is using the Covariance-Driven Stochastic Subspace Identification (SSI-COV). The analysis matrix **X** can directly be defined from the Toeplitz matrix (**T**) in SSI-COV:

$$\mathbf{X} = \mathbf{T} = \mathbf{Y_f}\ \mathbf{Y_p^T} \tag{10}$$

The system order for SSI-COV, Eq. (9) can also be applied.

The third one to define the analysis matrix is directly using the data Hankel matrix (trajectory matrix), and define the analysis matrix **X** as:

$$\mathbf{X} = \mathbf{Y}\,\mathbf{Y^T} \tag{11}$$

Based on the proposed three different analysis matrices, either null-space based damage index or subspace-based damage index can be calculated.

2.2 Damage Detection using Coupling of Singular Values from SSA

Singular spectrum analysis (SSA) is a novel technique and has proven to be a powerful tool for time data series analysis. It takes the singular value decomposition of data Hankel matrix embedded by the analyzed time data series and decomposes the data to several simple, independent and identifiable components. Basic capability of SSA includes finding trend, extracting periodic component, smoothing time series and de-noising of time series [11,12]. The basic procedure of SSA consists of four steps:

embedding, singular value decomposition, grouping and diagonal averaging. In the first step (embedding), the one dimensional time series is recast as an L-dimensional time series (trajectory matrix, same as Eq.(7). In the second step (singular value decomposition), the trajectory matrix is decomposed into a sum of orthogonal matrices of rank one:

$$\mathbf{Y} = \mathbf{U}\,\mathbf{S}\,\mathbf{V}^{T} \tag{12}$$

where **U** and **V** are orthogonal matrices and **S** is a diagonal real matrix such that its elements ($\sigma_1 > \sigma_2 > \sigma_3 > \cdots > \sigma_m$) are the singular values of the trajectory matrix **Y**. It is noted that the singular values of Y are the square root of the eigenvalues of **C** (**C**=$\mathbf{Y}^{\mathrm{T}}$ **Y**). These two steps constitute the decomposition stage of SSA. In the third and fourth steps, the components are grouped and the time series associated with the groups are reconstructed. The aim of this stage is to separate the additive components of the time series. It can be seen as separating the time series into two groups: the "signal" and the "noisy" components, which are by definition the components that are not interested in.

In SSA, if a periodic mode is encountered, each of which will be spitted into a pair of modes with high "degree of coupling", otherwise, the coupling effect is reduced. Here the "degree of coupling" is defined as:

$$\rho_k = \sigma_{2k-1} / \sigma_{2k} \qquad k = 1, 2, \cdots, n \tag{13}$$

where σ_i is the i^{th} singular value in singular spectrum analysis. If ρ_k parameters show an anomalous decreasing behavior the periodic mode collapse and the fact associated with different types of structural modes. Then, the loss of degree of coupling can be used of damage detection. In this study the coupling level between 1st and 2nd singular values in SSA are used for discussion because these two singular values represent most significant principal component in the analyzed time series. It is now defined the difference of the first two largest eigen values as one of the damage index (or Eigenvalue Difference Ratio, EDR):

$$DI_{v1} = (\sigma_1^2 - \sigma_2^2) / \sum_{i=1}^{L} \sigma_i^2 \tag{14}$$

If the difference between the 1st and 2nd singular value is small which indicates the principal component do exists in the analysis data. If the difference between the 1st and 2nd singular value is large different type of principal component has occurred. If the damage of a structural system can alter the dominant principal components, then high value of "DI_{vI}" may detect this change. It is important to note that in SSA the distribution of singular spectrum can also reflect the feature of signal; therefore, it can also be used as a measure of structural damage characteristics. The variation of singular spectrum can be defined as:

$$DI_{v2} = 1 - MAC(\mathbf{S}, \mathbf{S}_0) \tag{15}$$

where $\mathbf{S}_0$ is the distribution of singular spectrum from reference state (undamaged case) and $\mathbf{S}$ is the distribution of singular spectrum from analyzed state (damaged case), and *MAC* is defined as

$$MAC = \left| \sum_{q=1}^{L} \mathbf{S}(q)\mathbf{S}_0(q) \right|^2 \Big/ \sum_{q=1}^{L} \mathbf{S}^2(q) \sum_{q=1}^{L} \mathbf{S}_0{}^2(q) \tag{16}$$

Larger *MAC* value indicates the difference on the distribution of singular spectrum between reference state and analysis state is almost the same which means almost no damage between these two states.

The SSA reconstruction process can also be used for damage detection. Since the first two singular spectra values can represent a harmonic wave if the degree of coupling is strong enough, besides, it also represents the major principal component of the structural response. Therefore, the reconstruction process by using the first two largest eigenvalues from each time window can provide information on the change of principal component of the structural response. This change can be used for damage detection. Comparison on the root-mean-square value between the reconstructed data from the reference data and from the different moving time window, damage assessment can be performed.

2.3 Damage Detection using AR-ARX model

Different from using vibration measurement directly for damage detection, a model-based damage detection technique is also examined. Approaches based upon the statistical pattern recognition paradigm proposed by Sohn *et al.* [8] and extended by Lynch *et al*. [13] for on-line damage detection is discussed first. A two-stage prediction model, combining Auto-Regressive (AR) and Auto-Regressive with eXogeneous input (ARX) techniques, is constructed from the selected reference measurement as the undamaged model. The procedure is briefly described below:

a. Construct an AR model with *p* auto-regressive terms from a reference segment data *y(t)*:

$$y_m(t) = \sum_{i=1}^{p} \phi_i \, y_m(k-i) + r_{AR}^m(k) \tag{17}$$

where ϕ_i is the *i*-th AR coefficient, p is the order of the AR model. It is important to identify the suitable model order for the AR model. r_{AR}^m is the residual error and *m* indicates *m*-th time series. "m" sets of response data has to be collected, and a set of reference AR coefficients can be obtained for the structure. Based on these identified AR models, one can select a suitable one as a reference model. It is important to identify the suitable model order for the AR model.

b. With the selected "*n*-th" data set, the residual error, r_{AR}^n will be used as the background (or environmental signal) noise. Therefore, with this selected reference data set, an ARX model is employed to reconstruct the input/output relationship between r_{AR}^n and $y_n(t)$:

$$y_n(k) = \sum_{i=1}^{a} \alpha_i \, y_n(k-i) + \sum_{j=0}^{b} \beta_j \, r_{AB}^{n}(k-j) + \varepsilon_{ARX}^{n}(k) \tag{18}$$

where α and β are the coefficients of the ARX model, and *a* and *b* are the order of the ARX

model. The final residual error of the ARX model, ε_{ARX}^{n}, is defined as the damage sensitive feature of the structure. An extensive library of AR-ARX models, all of the same model size, corresponding to the undamaged structure is generated by exciting the structure with different levels of ambient excitation. One set of the ARX model coefficients and the standard deviation

of ε_{ARX}^{n} for the reference AR-ARX model will be used as the undamaged reference.

c. For the structure in an unknown state, a new set of ambient vibration data of the structure is measured. An investigation is made to determine how well the reference ARX(a,b) model can reproduce the input/output relationship of the residual error and the measurement $\tilde{y}(t)$:

$$\varepsilon_{\tilde{y}}(t) = \tilde{y}(t) - \sum_{i=1}^{a} \alpha_i \, y(t-i) - \sum_{j=0}^{b} \beta_j \, r_{AB}^{n}(t-j) \tag{19}$$

Note that the α_i and β_j coefficients are associated with the reference model.

d. Finally, the standard deviation of the ARX model residual error, $\sigma(\varepsilon_{\tilde{y}})$, using the newly measured data is determined. The estimated standard deviations of $\varepsilon_{\tilde{y}}(t)$ and $\varepsilon_{ARX}^{n}(t)$ is then calculated and is defined as the damage sensitive feature. If the ratio of $\sigma(\varepsilon_{\tilde{y}})/\sigma(\varepsilon_{ARX}^{n})$ becomes larger than some threshold value h(>1), then the system is considered to have undergoes some structural system changes. This algorithm can be applied for on-line damage detection.

2.4 Damage Detection Using Damage Sensitivity Factor

Since damage detection can be demostrated through the analysis of measurement directly from response vibration signals of a structure before and after damage, therefore, either single-variant or multivariate auto-regressive (AR) time series can be used to model the vibration data obtained from the sensor. In general, the AR coefficients provide information about the system natural frequencies and the damping ratios. Consider the single-input and single-output (SISO) case as shown in Eq.(17), the method of least square can be applied to estimate model parameters. Nair *et al.* [14] reported that the Damage Sensitivity Factor (*DSF*) depending on the AR coefficients is the most promising because these coefficients are statistically the most significant among all the coefficients of model for damage detection. The *DSF* is defined as:

$$DSF_{acc,1} = \frac{|\alpha_1|}{\sqrt{\alpha_1^2 + \alpha_2^2 + \alpha_3^2}} \tag{20}$$

Different from the SISO AR model, to determine the multivariate AR coefficients, the multivariate AR model is considered:

$$\{y(t)\} + [\alpha_1]\{y(t-1)\} + [\alpha_2]\{y(t-2)\} + \ldots + [\alpha_p]\{y(t-p)\} = \{e(t)\} \tag{21}$$

$$\text{Or} \quad \{y(t)\}_{d\times 1} = [A]_{d\times dp}\{\varphi(t)\}_{dp\times 1} + \{e(t)\}_{d\times 1}$$

where $[A]_{d\times dp} = [-[\alpha_1]-[\alpha_2]\ldots-[\alpha_i]\ldots-[\alpha_p]\ ]$ is the model parameter matrix, d is the number of sensing nodes, p is the order of the AR model, $[\alpha_i]_{d\times d}$ is the matrix of autoregressive parameters relating the output $\{y(t-i)\}$ to $\{y(t)\}$, $i=1{:}p$, and $\{\varphi(t)\}_{dp\times 1} = \begin{Bmatrix} \{y(t-1)\}_{d\times 1} \\ \{y(t-2)\}_{d\times 1} \\ \ldots \\ \{y(t-p)\}_{d\times 1} \end{Bmatrix}$ is the regressor for the output vector $\{y(t)\}$, $\{y(t-i)\}_{d\times 1}$ (i=1:p) is the output vector with delay time $i\times T_s$, T is the sampling period (s), and $\{e(t)\}_{d\times 1}$ is the residual vector of all output channels, and considered as the error of the model.

If (N ≥ dp+d) consecutive output vectors of the responses from $\{y(k)\}$ to $\{y(k+N-1)\}$ are taken into account, the model parameters can obviously be estimated with the least squares method by minimizing a norm of error sequences. The data matrix is first constructed from N successive samples [15,16]:

$$[K]_{N\times(dp+d)} = \begin{bmatrix} \{\varphi(t)\}_{dp\times 1}^T & \{y(t)\}_{d\times 1}^T \\ \{\varphi(t+1)\}_{dp\times 1}^T & \{y(t+1)\}_{d\times 1}^T \\ \ldots & \ldots \\ \{\varphi(t+N-1)\}_{dp\times 1}^T & \{y(t+N-1)\}_{d\times 1}^T \end{bmatrix} \tag{22}$$

The QR factorization of the data matrix $[K]_{N\times(dp+d)} = [Q]_{N\times N}[R]_{N\times(dp+d)}$ can be computed by using the Householder method [17] or Givens rotation [18]. It gives $[Q]_{N\times N}$ which is an orthogonal matrix $(Q.Q^T = I)$ and $[R]_{N\times(dp+d)}$ which is an upper

triangular matrix with the form:

$$[R]_{N\times(dp+d)} = \begin{pmatrix} [R_{11}]_{dp\times dp} & [R_{12}]_{dp\times d} \\ 0 & [R_{22}]_{d\times d} \\ 0 & 0 \end{pmatrix} \tag{23}$$

The *QR* factorization of the data matrix *K* leads to the Cholesky factorization

$$\Gamma = K^T K = R^T R$$

$$R^T R = \begin{pmatrix} [R_{11}^T][R_{11}] & [R_{11}^T][R_{12}] \\ [R_{12}^T][R_{11}] & [R_{12}^T][R_{12}]+[R_{22}^T][R_{22}] \end{pmatrix} \tag{24}$$

The model parameters matrix $[A]_{d\times dp}$ is calculated from the Cholesky factorization:

$$\begin{aligned} [A] &= ([R_{12}^{\mathrm{T}}][R_{11}]) \cdot ([R_{11}^{\mathrm{T}}][R_{11}])^{-1} \\ &= ([R_{11}^{-1}][R_{12}])^{\mathrm{T}} \end{aligned} \tag{25}$$

and the estimated covariance matrices of the unnoised part $[D]_{d\times d}$ and of the error part $[E]_{d\times d}$ can be estimated via the computation of the QR factorization as follows[19]:

$$\begin{aligned} [D]_{d\times d} &= [R_{12}^T][R_{12}] \\ [E]_{d\times d} &= [R_{22}^T][R_{22}] \end{aligned} \tag{26}$$

Once the model parameters are estimated, the state matrix of the system can be established in the form of autoregressive parameters [20]:

$$[\Phi]_{dp\times dp} = \begin{bmatrix} -[\alpha_1]_{d\times d} & -[\alpha_2]_{d\times d} & -[\alpha_i]_{d\times d} & \cdots & -[\alpha_p]_{d\times d} \\ I & 0 & 0 & \cdots & 0 \\ 0 & I & 0 & \cdots & 0 \\ \cdots & \cdots & \cdots & & \\ 0 & 0 & 0 & I & 0 \end{bmatrix} \tag{27}$$

where the poles of the model are also the root of the characteristic polynomial of the state matrix.

Since the model is updated with respect to its system order, it is appropriate to use stabilization diagrams to identify the stable system natural frequencies. By observing the stability of the identified frequencies with respect to increasing model order, it is possible to distinguish the physical modes from the spurious modes.

3. EXPERIMENTAL SETUP FOR DAMAGE DETECTION

To discuss the above mentioned damage detection algorithms the failure of bridge structure during scouring process is examined. In this example an experimental testing on a bridge model subjected to scouring test. A four span bridge model with simply

supported girder on each pier was constructed to across a flume of width 4.5 meter in the hydraulic lab. The span length is about 1.0 m. The sketch and the dimension of this bridge are shown in Figure 1. The bridge piers are embedded in sand with depth of 30 cm. 12 velocity sensors are deployed along the bridge deck to collect the vibration signal of the bridge during scouring process in transverse direction (along stream line). The scouring test runs for about 3 hours. To focus the major scouring phenomenon on one single bridge pier, the major running stream water was guided and focuses the scouring effect mainly on the 3rd pier between sensor number 9 and 10. Photos of the bridge test setup and the scouring test are shown in Figure 2. Velocity response data of the bridge during scouring process are collected. The VSE-15D sensor is used and it is a servo velocity meter produced by Tokyo Sokushin Co., Ltd. This sensor is very sensitive to detect the low level vibration motion and the linear range (0.2Hz~70Hz) is suite for SHM applications. Data acquisition system collected all the velocity response of the bridge from all twelve sensors with sampling rate of 200 Hz. Figures 3a and 3b show the collected velocity response from sensor node #2 and node #9. The total run time on this bridge scouring test is 200 min. (12,000 sec). The response data from all sensing nodes (12 sensors) can be used for on-line monitoring of the bridge structure. As shown in Figure 3, at pier 3 the laying depth (embedment depth of sand, i.e. 30 cm) significantly reduced at the beginning of the incoming water as compare to the other piers. From the observation of the recorded time data, at *t=5800* sec and *t=7500* sec there are two significant changes of vibration measurement were observed from sensor node No.9. This abnormal response data is due to the settlement of pier No.3.

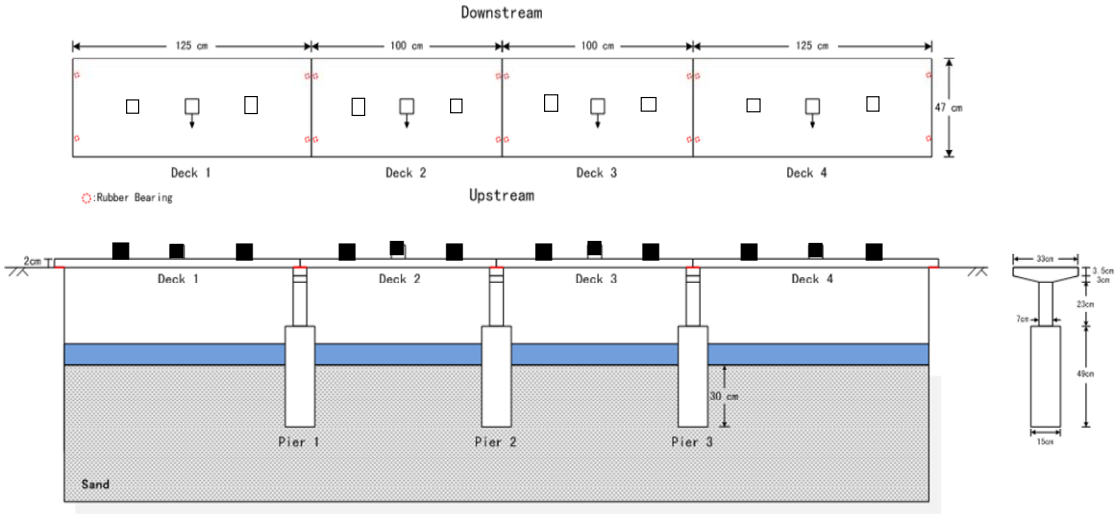

Figure 1: Sketch and dimension of the model bridge for testing.
The locations of sensors on the deck are also shown.

3.1 Results using null subspace-based damage identification

Three different analytic matrices were introduced in section 2 which can be used to calculate the damage indices: SSA-based, SSI-DATA based and SSI-COV based.

(a)

(b)

(c)

Figure 2: Photos of the bridge scouring test in the hydraulic laboratory; (a) test setup, (b) during the scouring test, (c) after the scouring test.

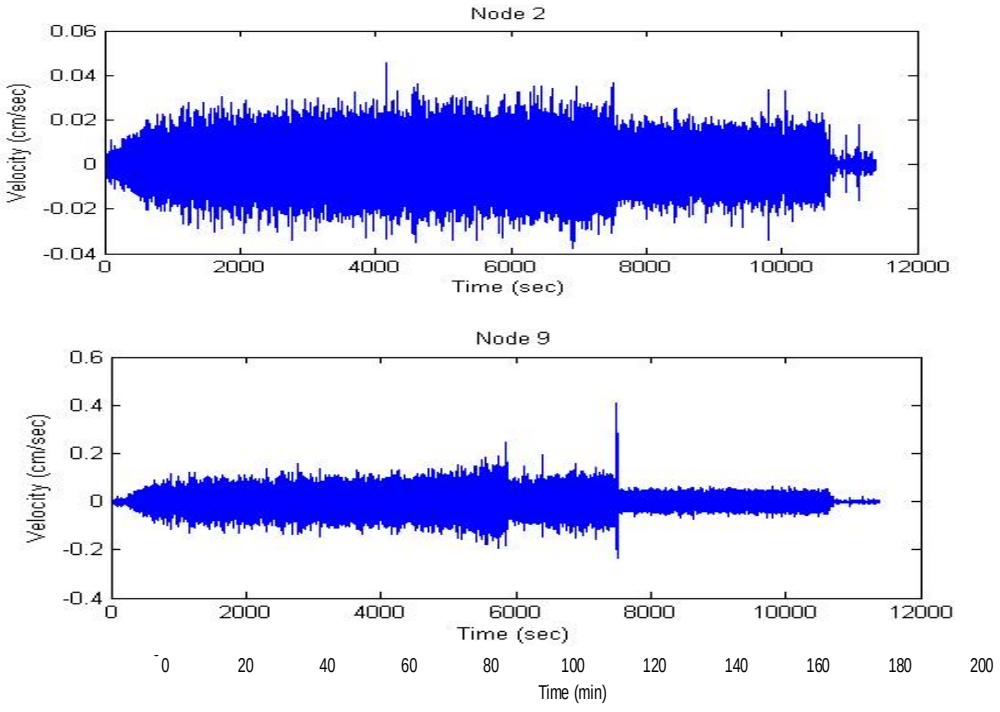

Figure 3: Velocity response from sensing nodes 2 and 9.

Damage Identification from bridge scouring test Before conducting the damage assessment, in order to have a better understanding on the bridge behavior during scouring, a multivariate recursive data-driven stochastic subspace identification technique (RSSI-DATA) is used to identify time-varying system natural frequencies of the bridge [21]. ***Figure 4*** shows the time-varying system natural

frequencies of the bridge system. It is clearly observed that the change of system natural frequencies is more focus on some fundamental modes and is in consistent with the abnormal change of response measurement. The identified time-varying system natural frequencies will be served as the reference to compare with the extracted damage features by using the proposed damage detection methods.

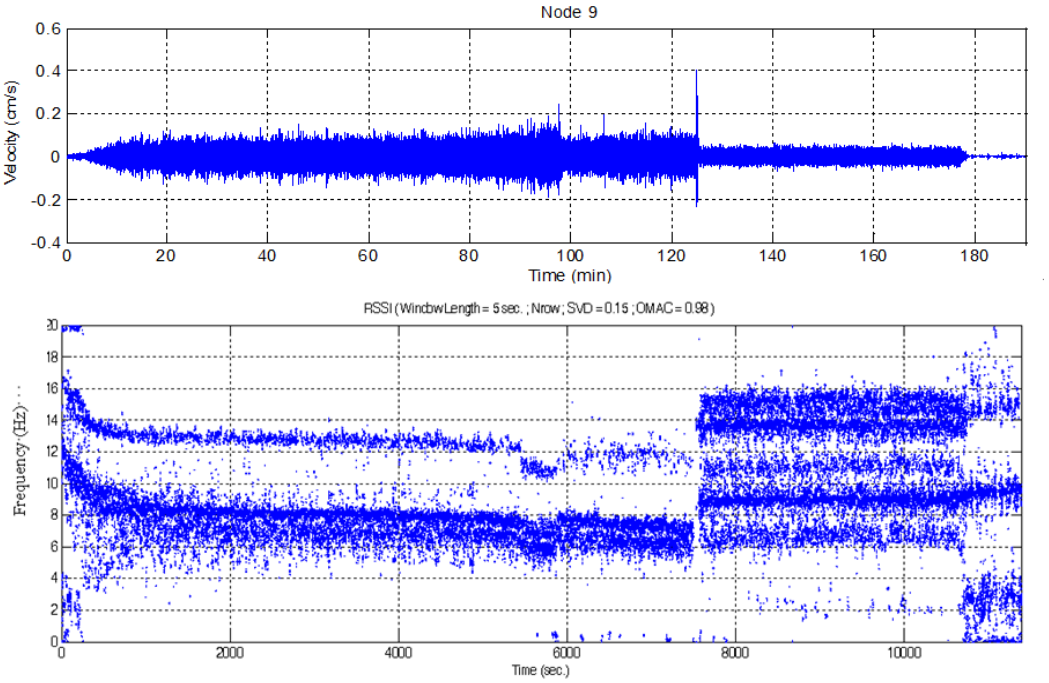

Figure 4a: Plot the comparison between the identified time-varying system natural frequencies (using SSI-DATA method) and the recorded response (from sensor node 9) of the bridge during scouring process.

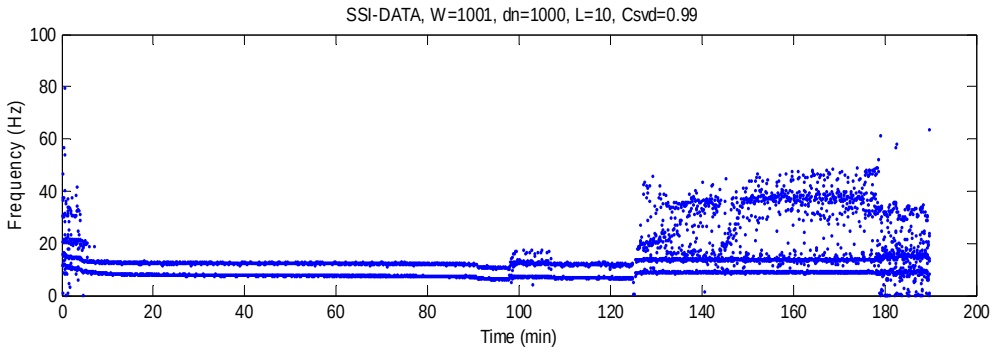

(a) Identified time-varying system natural frequencies with C_{svd}=0.9999

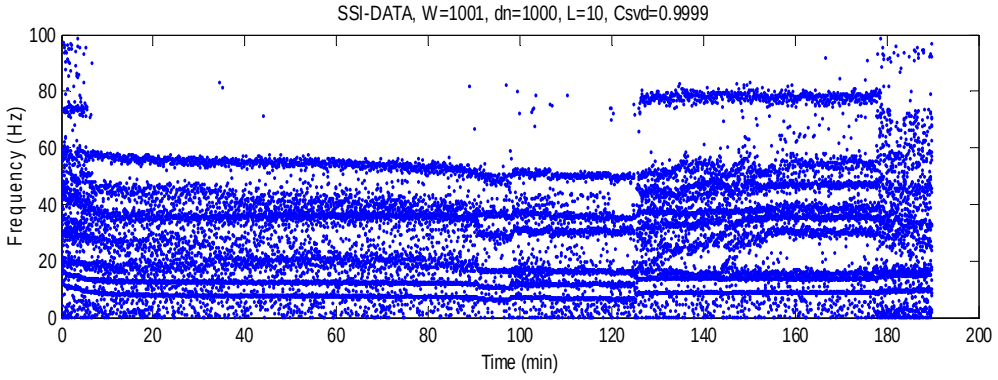

Figure 4b: System identification result of scouring test data with different C_{svd} (SSI-DATA algorithm using data from all 12 sensors)

In this case study, L=100 is used in data Hankel matrix and select C_{SVD}=0.99 to calculate DI_N and DI_S by using SSI-DATA based algorithm. Through moving window technique, Figure 5 shows the estimated time-varying damaged indices (DI_N and DI_S) by using response data from sensors on different deck. It is observed that no matter which data set was used, both indices can identify the damage situation. The estimated damage indices from data set on deck 3 and on deck 4 show larger damage indices than other set of data because the significant damage of pier 3 can influence sensing data on both deck 3 and deck 4. The result is inconsistent with the identified time-varying system natural frequencies.

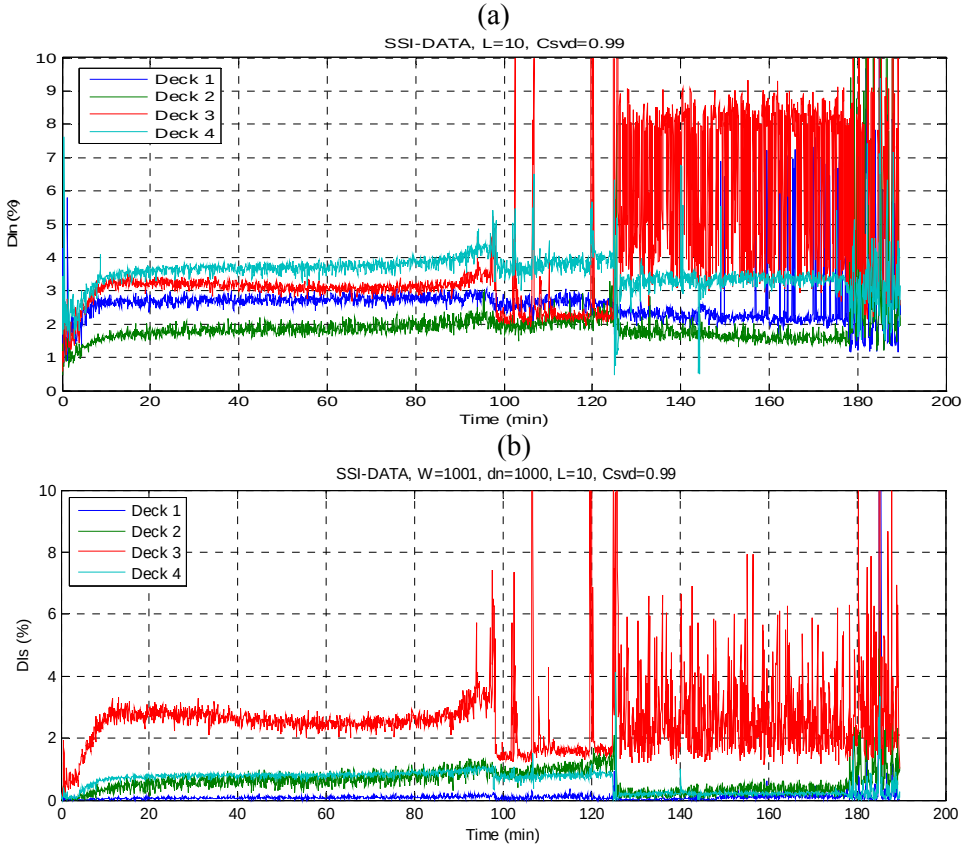

Figure 5: Estimated time-varying damage indices from different set of sensing data; (a) Null space damage index, (b) Subspace- based damage index.

3.2 Results using degree of coupling from SSA

Damage Identification from bridge scouring test Different from the damage scenario of the 6-story steel frame, the damage identification of bridge scouring will focus on low frequency damage. With the concept of moving window (window length=40 sec) the data Hankel matrix was formed from each time window by using either from individual sensing node or from all recorded sensing nodes. Figures 6a and 6b show the difference between the first two largest eigenvalues by using data from single measurement (sensing node 2 and node 9, respectively). Larger difference indicates poor degree of coupling. This two figures show that prior to the significant settlement of the bridge pier No.3 after *t=7800 sec*, the distinct feature of the difference between two largest eigenvalues can be identified at about *t=5800 sec*. This feature can be served as an index for early warning. The difference on the first two

largest eigenvalues can also be calculate from all set of measurements instead of using data from a single sensing node, as shown in Figure 6c (plot in log scale). The result is even more promising for early warning.

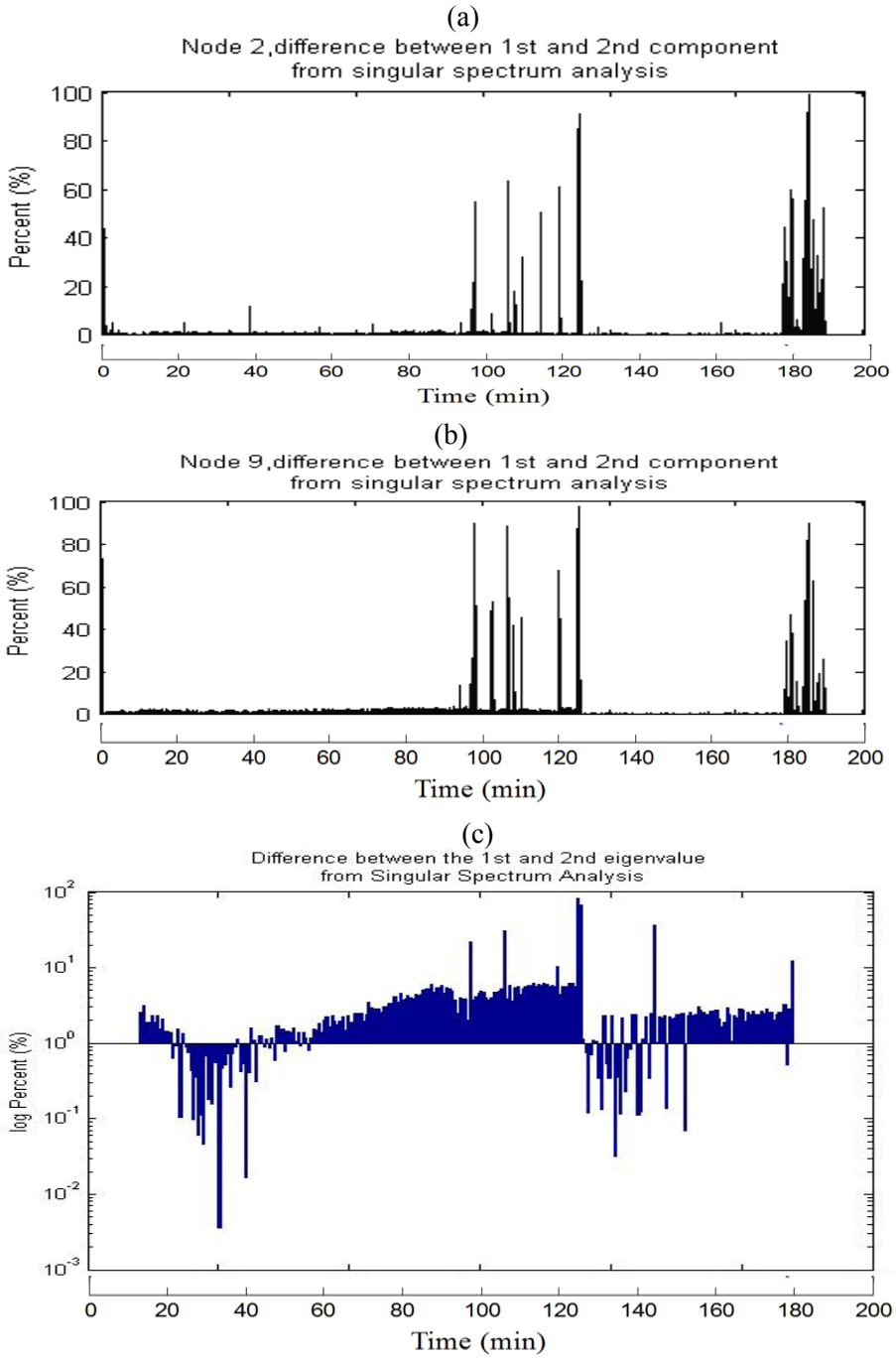

Figure 6: Difference between the 1st and 2nd eigenvalue-ratio from Singular Spectrum Analysis, (a) using single measurement from sensing node 2, (b) using single measurement from sensing node 9,(c) using all set of measurements.

In cooperated with moving window technique (each window with 40 sec), the reconstruction process of signal by using only the first two largest eigenvalues from SSA can be generated. Conduct this process in each moving time window. Then by selecting the original reconstructed signal as reference (or undamaged case), and comparison on the root-mean-square (RMS) value between the original signal and the newly reconstructed signal (through moving window technique) can be made. The

RMS error between the reconstructed and original recorded signal (the first time window) is plotted and shown in Figures 7a and 7b. It is observed that the RMS error of the sensor signal from different sensing nodes shows a significant change at around *t=5800* sec before the large settlement occurred. Besides, if the selected sensing node is more close to the damage location, larger RMS value can be observed. As shown in Figure7b the RMS value from sensing node 10 shows the largest. This information can also be used as an index for damage detection as well as provides an early warning message.

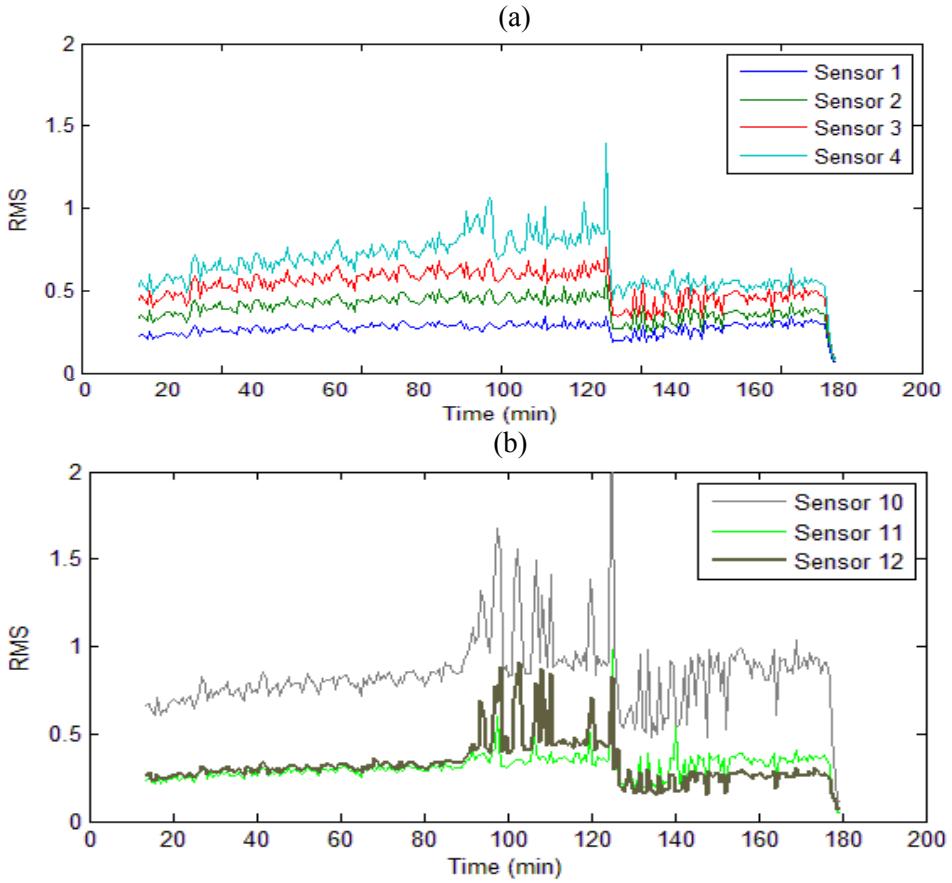

Figure 7: Plot of RMS error between the measurement and the prediction using the reconstruction signal (from the two largest eigenvalues) of SSA; (a) From sensing nodes 1,2,3, and 4; (b) from sensing nodes 10, 11 and 12.

3.3 Results from using AR model for damage detection

Damage Identification from bridge scouring test Estimation of *DSF* value from the bridge scouring test data can be applied by using either single-variate or multivariate AR model. The order of 40 is selected for using the single-variate AR model. With the consideration of system damping ratio less than 10% to select the system poles, Figure 8a shows the time-varying *DSF* value. Although the computation still contains spurious modes (with order of 40), the results are noticeable to indicate the significant change at t=95 min. and t=125 min. The analysis of using multivariate AR model is also applied. The order of multivariate AR model is set to 8 (using data from all sensing nodes) and every mode with damping ratio less than 20 % is

considered to calculate the *DSF,* as shown in Figure 8b. The change of DSF at t=95 min. shown in this figure is even more clear to be identified than using only singlevariate AR model.

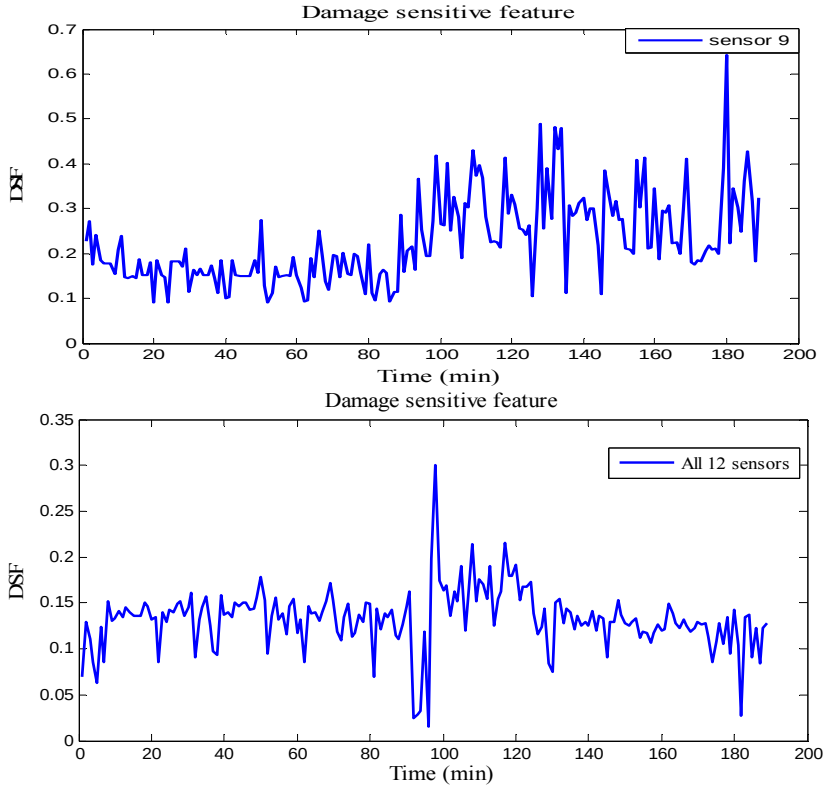

Figure 8: (a) Damage sensitive feature using data from sensor 9 using AR model of order 40 and damping ratio below 10%
(b) Damage sensitive feature using data from all sensors using AR model of order 8 and damping ratio below 20%

For the distributed sensing system on long extended structure, such as monitoring the bridge vibration, the two-tier AR-ARX model can also be used for damage detection. A reference database corresponding to the undamaged structure needs to be defined. It is assumed the initial 80 min. sequences of data (each with time window of 40 seconds), from the recorded response are selected as the undamaged (reference) data. Once the reference database is established, an AR-ARX model pair is fitted using the response data. Following the procedures discussed in the previous section, with the new appending data the ratio of AR-ARX two-tier model residual errors can be generated for each moving time window. The difference on the residual error is attributed to the difference between the current state of measurement to the reference state. As shown in Figure 9, the residual error starts to increase at t=80 min. and then follows at t=95 min. and 125 min. The increase of residual error at these three different specific times is in consistent with the time when the change of dynamic characteristics of the bridge structure occurred. Using data from different sensing node (i.e. Node 10, Node 11, or Node 12) to calculate the residual error can also get the same result.

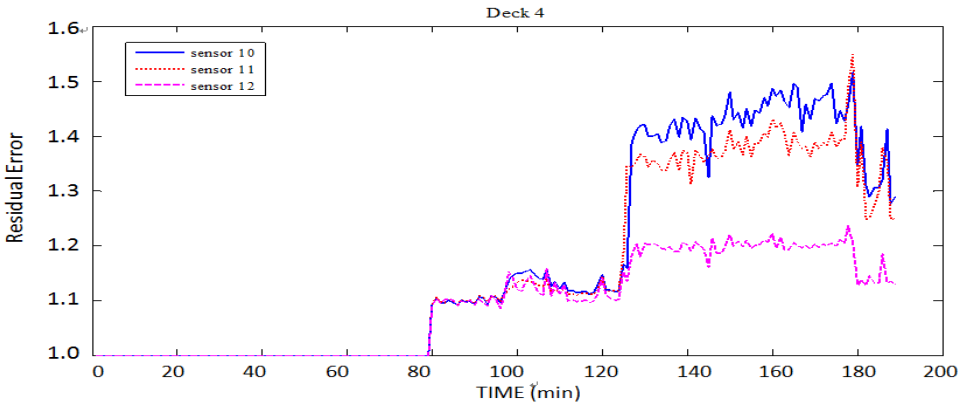

Figure 9: Plot of time-varying residual error from the two-tier AR-ARX model.

4. Bridge Monitoring Using Eigenvalue Ratio Difference (ERD): Niu-Dou Bridge

Description of the Niu-Dou Bridge test

Niu-Dou Bridge is located at Yi-Lan County across Lan-Yang River. It is comprised of two independent bridges at the upstream side and the downstream side. The upstream side bridge is older than the downstream side one. They are both the simple support reinforced concrete bridges with 7 spans. Each span is 36.6m. The pier height is about 10.5m. Photos of Niu-Dou Bridge are shown in Figure 10. The upstream side bridge suffered severe scouring and the impact from debris flow during the typhoon season, and its foundations were repaired and strengthened many times in the past. Niu-Dou Bridge is considered as a dangerous bridge by the authority. The authority always closed the bridge during the typhoon strike for safety and planed to dismantle the bridge in 2011.

Starting from April 2010 velocity response data of the upstream side bridge are collected. VSE-15D sensor was used and the data was transferred through wireless communication mechanism. The illustration of the sensor location and number are shown in Figure 10. All sensors are installed upon the bridge deck. Both the vertical and transverse direction velocity responses were collected. It includes the general measurement at 2010/04/08, 2010/06/09, 2010/07/23 and 2010/10/12, and the data during Fanapi Typhoon strike at 2010/09/19 ~ 2010/09/21. The transverse velocity responses measured from locations of D5 was used for discussion. Figure 11(a) shows the horizontal velocity time history from sensor at D5. The response amplitude is larger during the typhoon strike resulting from the wind and high water level during the typhoon strike. The main objective of the analysis is to study the applicability of using *ERD* indicator to identify the abnormal condition of the bridge during the typhoon strike.

Analysis Result

First, the short-time Fourier transform was used to realize the frequency content of the measured response. **S**pectrogram of the recorded velocity time history was studied (from D5 sensor node), as shown in Figure 11a.

(a)

(b)

(c)

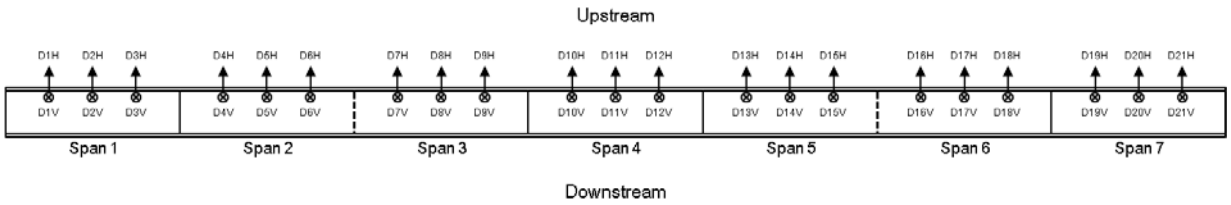

Figure 10 Photos of Niu-Dou Bridge (a) before and (b) during typhoon strike and (c) the illustration of the sensor location and number

The window length is 5sec and the hamming window function is used. It is found that there are several main differences between the normal condition (data measured at 2010/04/08, 2010/06/09, 2010/07/23 and 2010/10/12) and abnormal environmental conditions (data measured during Fanapi Typhoon strike at 2010/09/19 ~ 2010/09/21):

1. Under normal environmental condition, the spectrogram property is stable (time-invariant). The vibration mode at about 3Hz is always dominant. The modal frequency is not time-variant.
2. Under abnormal environmental condition (Typhoon condition), the spectrogram property is unstable and variant with time. For example, the dominant vibration mode changes from about 3Hz mode to 7.5Hz mode for 9/19 D5H data, and higher mode vibration with frequency between 10Hz to 20Hz is excited for 9/20 D5H data.
3. The observed signal frequency is different for different sensor location. This

(a)

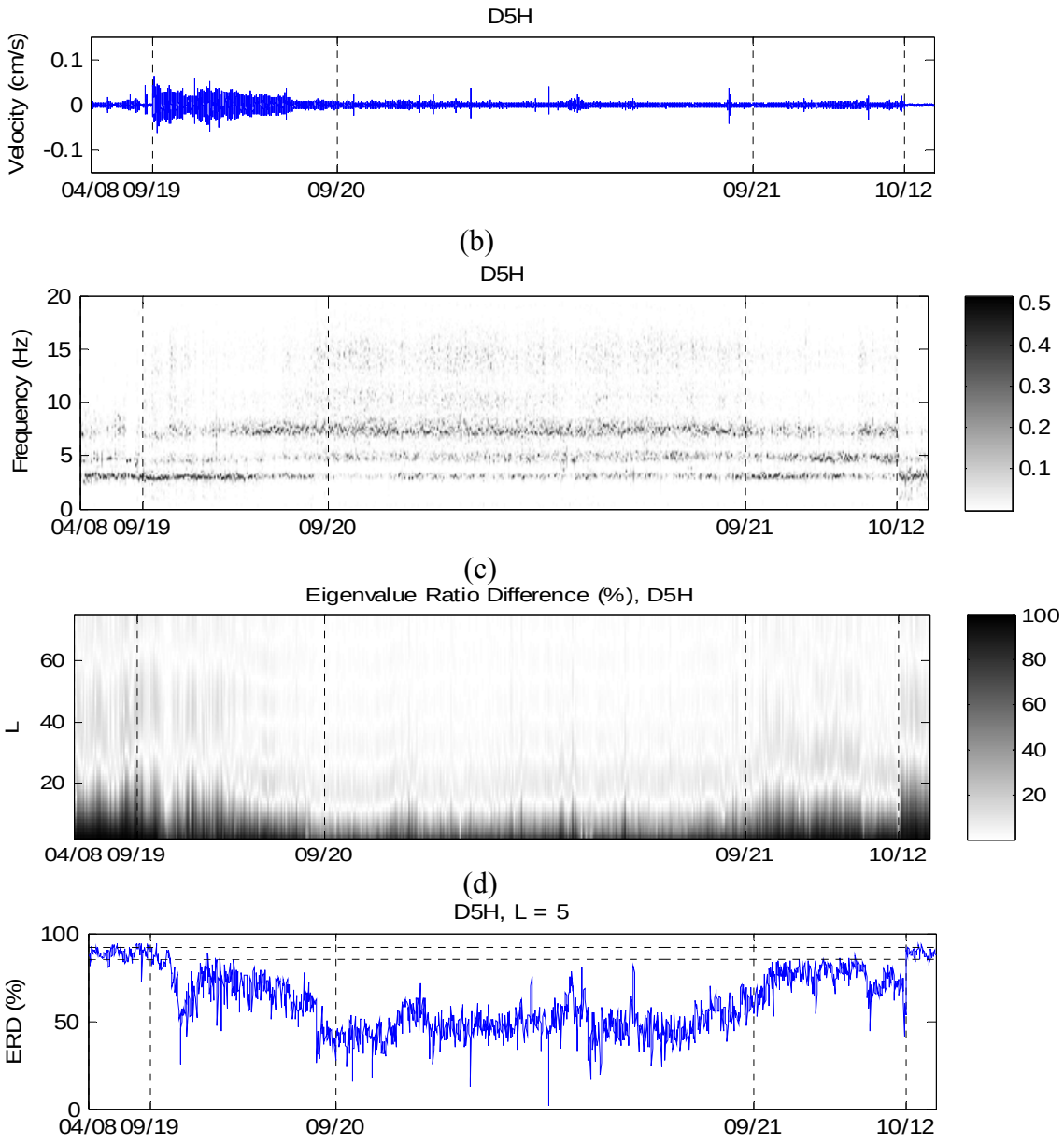

Figure 11 (a) Measured velocity response at D5H of Niu-Dou Bridge; (b) Short-time Fourier transform of measured horizontal velocity response at D5H; (c) Eigenvalue ratio difference of measured horizontal velocity response at D5H; (d) Eigenvalue ratio difference of measured horizontal velocity response at D5H for L=5.

may result from the large and complex structural system, which may induce the local vibration mode.

4. Time-varying system frequency can be found from the measurement in 9/20 (during typhoon) at D11H. The vibration mode with frequency 3Hz decreases to 2.5Hz and gradually returns to 3Hz again.

Based on the above observation, we believe that the bridge dynamic characteristics may change resulting from abnormal environmental condition. However, we cannot point out the causes of this abnormality definitely. This abnormality may result from either the nonlinearity, damage of the bridge structure, applied force characteristics, the scouring of the bridge pier, etc. Other monitoring

information is still needed to realize the real condition of the bridge.

Figure 11(c) shows *ERD* result of the velocity time history for different sensor locations in transverse direction for sensor location D5. The rectangular window is used and the window length is 5sec. *ERD* result is stable from the measurements under normal condition, and variation of critical length can be observed from the measurements in abnormal environmental condition during 9/19 to 9/21. Figure 19(d) shows *ERD* result for the row size of Hankel matrix equal to 5 for sensor location D5. This figure also shows two y-axis grids which present the mean plus and minus one standard deviation of *ERD* result for the general measurement before the typhoon strike. The dramatic time variation can still be observed for the abnormal environmental condition during 9/19 to 9/21. For example, *ERD* of D5H sensor is equal to about 90% before and after typhoon strikes. However, its variation from 40% to 90% can be observed during typhoon strike. *ERD* result before the typhoon strike is a little different to *ERD* result after the typhoon strike for different sensing node. It means that the bridge system may have permanent change or damage after the typhoon strike. In contrast to spectrogram result, *ERD* result provides more clear information about the variation of bridge characteristics during the typhoon strike.

REFERENCES

1. Doebling, S., Farrar, C., Prime, M., and Shevitz, D., Damage identification and health monitoring of structural and mechanical systems from changes in their vibration characteristics, *Tech. Rep. LA-13070*, Los Alamos National Laboratories, Los Alamos, NM. 1996.
2. Staszewski, W., Gearbox vibration diagnostics – an overview, *Proceedings of the 8-th OMADEM-96)*, Sheffield, England, 16-18, July. 1996.
3. Ruotolo, R., and Surace, C., Using SVD to Detect Damage in Structures with Different Operational Conditions. *Journal of Sound and Vibration*, Vol. 226, No. 3, 1999.
4. Yan, Ai-Min and Jean-Claude Golinval, Null subspace-based damage detection of structures using vibration measurements, *Mechanical Systems and Signal Processing*, Vol: 20, 611–626, 2006.
5. Broomhead, D.S., King, G.P., “Extracting qualitative dynamics from experimental data,” *Physica D: Nonlinear Phenomena,* 20 (2-3), 217–236, 1986
6. Broomhead, D.S., Jones, R., King, G.P., Pike, E.R. (1987), “Singular system analysis with application to dynamical systems,” In E.R. Pike and L.A. Lugaito, editors, Chaos, Noise and Fractals, pages 15–27. IOP Publishing, Bristol, 1987.
7. Bozzo, E., Carniel, R., Fasino, D., Relationship between Singular Spectrum Analysis and Fourier analysis: Theory and application to the monitoring of volcanic activity, *Computers and Mathematics with Applications*, 60 (3), 812-820, 2010.
8. Sohn, H., Farrar, C.R., “Damage diagnosis using time series analysis of vibration

signal," *Smart Materials and Structures*, 10 (3), 446-451, 2001.

9. Nair, K. K., et al., Time series-based damage detection and localization algorithm with application to the ASCE benchmark structure. *J. Sound Vib., 291*(2), 2006.
10. Naira, K. K., & Kiremidjian, A. S., Damage Diagnosis Algorithms for Wireless Structural Health Monitoring. Ph.D. Thesis, Stanford University, Stanford, USA, 2007.
11. Golyandina, Nina; Nekrutkin, Vladimir; Zhigljavsky, Anatoly. Analysis of time series structure: SSA and related techniques. Boca Raton, Fla. : Chapman & Hall/CRC, 2001
12. Alonso, F.J., Del Castillo J.M., and Pintado P. Application of singular spectrum analysis to the smoothing of raw kinematic signals. *Journal of Biomechanics*, 38(5): 1085- 1092, 2005.
13. Lynch, J. P., Sundararajian, A., Law, K. H. and Kiremidjian, A. S., Kenny, Thomas and Carryer,

    Ed, Computational Core Design of a Wireless Structural Health Monitoring system, *Proc. of Advances in Structural Engineering and Mechanics* (ASEM'02), Pusan, Korea, August 21~23, 2002.
14. Noh, Hae Young, K. Krishnan Nair, Anne S. Kiremidjian, and C. H. Loh, Application of time series based damage detection algorithms to the benchmark experiment at the National Center for Research on Earthquake Engineering (NCREE) in Taipei, Taiwan, *Smart Structures and Systems*, Vol. 5, No. 1, 95-117, 2009.
15. Vu, V. H., et al., *Multi-autoregressive model for structural output only modal analysis.* Paper presented at the Proceedings of the 25th Seminar on Machinery Vibration, St.John, Canada, October, 2007.
16. Vu, V. H., et al. Operational Modal Analysis of non-stationary Mechanical Systems by Short-time Autoregressive (STAR) Modelling. *Proceedings of the 3rd International Conference on Integrity*, Reliability and Failure, Porto, Portugal, 2009.
17. Golub, G. H. and Van Loan, C. F. Matrix Computations. 3rd Ed. The Jhons Hopkins University Press, Baltimore, Maryland, p. 70. 1996.
18. Bjorck, A. (Ed.). *Numerical Methods for Least Squares Problems*. Philadelphia: Society for Industrial and Applied Mathematics, 1996
19. Vu, V. H., et al., Operational modal analysis by updating autoregressive model. *Mechanical Systems and Signal Processing, 25*(3), 1028-1044, 2011.
20. Pandit, S. M., *Modal and spectrum analysis: data dependent systems in state space*. New York, N.Y.: J. Wiley and Sons, 1999.
21. Loh, C.H.; Weng, J.H.; Liu, Y.C.; Lin, P.Y. and Huang, S.K., Structural damage diagnosis based on on-line recursive stochastic subspace identification, *Smart Materials and Structures,* V.20, No.5, 2011, 055004 (10pp).